DETAILED STUDIES OF ISOTOPES OF PRASEODYMIUM AND CERIUM OF MASS 137

by

Gordon T. Danby, B.Sc.

A thesis submitted to the Faculty of Graduate Studies and Research of McGill University in partial fulfilment of the requirements for the degree of Doctor of Philosophy

Radiation Laboratory Department of Physics

April, 1956

ACKNOWLEDGMENTS

The author wishes to express his appreciation for the encouragement given and for the invaluable direction and originality of thought which were provided at all times by Dr. J.S. Foster, F.R.S., Director of the Radiation Laboratory.

He is also appreciative of the efforts of Dr. A.L. Thompson of the Radiation Laboratory staff, who assisted in the direction of the project, and whose interests ranged beyond the chemistry to all facits of the work.

The author further wishes to express his gratitude to Dr. H.M.

Skarsgard for his advice in the use of γ-ray spectrometers and help in the measurement of coincidences, and to Dr. R.E. Bell and Dr. D.

Jackson for their advice on various problems of nuclear spectroscopy.

Thanks are also due to Mr. F. Carter who assisted in the experiments on the multiple filament and resolution of the mass spectrometer, to Mr. R.H. Mills for his cooperation in obtaining cyclotron bombardments, and to Mr. S. Doig for the unlimited use of the machine shop facilities.

SUMMARY

Extensive modifications to a small mass separator, including a new radial lens system and collection mechanism, have improved the purity and efficiency of separation.

Studies of mass separated isotopes have confirmed definitely the existence of 1.5 hr Pr¹³⁷ and 1.0 hr Pr¹³⁶. The branching ratios and characteristic Y-rays of Pr¹³⁹, Pr¹³⁸, Pr¹³⁷, and Pr¹³⁶ were obtained. The decay of Pr¹³⁷ to a 9.0 hr state of Ce¹³⁷ was discovered.

A new 34.4 hr isomeric state in Ce¹³⁷ was discovered, decaying by a 254.5 kev (14) transition to the 9.0 hr ground state. This decays by electron capture to the ground state of La¹³⁷, except for a 25 branching to a 440 kev (E2) excited state. A very weak 0.65 branching was found from the 34.4 hr isomeric state directly to a complex series of about 800 kev levels in La¹³⁷. The lower limit for the half-life of La¹³⁷ was increased to 1 x 10⁶ years.

TABLE OF CONTEMES

	Page
ACKNOLLEDGELENTS	(i)
SUMCIRY	(ii)
INTRODUCTION	1
PART A. IMPROVENENTS IN THE MASS SPECTROGRAPH	3
1. The Main Features of the Mass Spectrograph	3
2. The Characteristics of the Ion Source	5
3. Investigations of Lens Systems	\$
(a) The Potential Supplies	3
(b) The Original Lens System	5
(c) The New Lens Components	10
(d) Some Principles of Ion Optics	13
(e) The New Lens System	13
I_{i} . Studies of the Surface Ionization Effect	13
5. The Multiple Filament	22
6. The Resolution	23
7. The Collector	26
3. Summary and Discussion	30
BIBLIOGRAPHY	33

PART	Р.	A DETAILED STUDY OF ISOTOPES OF PRASEODYMIUM AND CERIUM OF	MASS	137.
I.	a St	urvey of Previous Mork	34	
II.	The	Irradiations and Chemical Separations	36	
	(a)	The Targets	36	
	(b)	The Chemical Separations	37	
		(i) Lanthanum Targets		
		(ii) Cerium Targets		
III.	Sout	rce Preparations	41	
īv.	Stu	dies on Praseodymium Isotopes in the Mass 137 Region	43	
	(a)	The Mass Separations	43	
		(1) Separations and Detections	43	
		(2) The Results	46	
	(b)	The Conversion Electron Spectrum	51	
	(c)	Conclusions and Analysis of Results	52	
٧.	Stud	dy of Cerium Formed from Praseodymium Decay	56	
	(a)	Gamma-ray Spectrum	56	
	(b)	The Conversion Electron Spectrum	57	
	(c)	Calculations and Discussion	53	
	(d.)	Conclusions	61	
VI.	Stud	dy of Cerium 137 Produced by Proton Reactions on Lanthanum	62	
	(a)	The Gamma-ray Spectrum	62	
	(b)	The Conversion Electron Spectrum	64	
		(1) The Thin-Lens Spectrometer Results	64	
		(2) The 180° Spectrograph Conversion Results	65	
VII.	Inv	vestigation of Coincidences	68	
	(a)	The 440 kev γ-ray	69	
	(b)	The 255 kev γ-ray	70	
	(c)	Conclusions	71	
VIII.	. 1	Proposed Decay Scheme for the M 137 Chain	7 2	

BIBLIOGRAPHY

76

INTRODUCTION

The mass separation of the radioactive isotopes of an element is often an essential preparation for a study of the radiations. When neighbouring isotopes have similar disintegration periods, the assignment of observed radiations to a particular isotope is otherwise difficult. Accurate yield curves, or cross bombardment with different particles, can make assignments more probable. Careful "milking off" of daughter activities by chemical means may also be very helpful. However, if an element is chemically separated from other elements, and then separated into its various mass components on thin foil, any observed properties of a single mass cut from the foil may be definitely assigned to a particular isotope or its decay products.

The value of this technique may be reduced by certain limiting factors. Obviously, the life of the active isotope must survive a complex process of preparation and analysis. The need for pure elementary sources of high specific activity often raises difficult chemical problems. Moreover, the efficiency of ion production from the hot filament source usually employed in mass spectrographs is commonly so low that the surviving activity gives only the period of decay and a few radiations under low resolution. Even so, this information may prove essential to the assignment of high resolution data from relatively strong sources of unseparated isotopes.

Thus owing to the importance of mass analysis, the first portion of the present research was devoted to improvements in the efficiency of a small mass spectrograph which had proved useful in earlier investigations.

Since an investigation at Oak Ridge (Handley et al. 1954) failed to confirm the discovery of Pr^{137} by Dahlstrom (1953) in this Laboratory, the neutron deficient isotopes of Praseodymium were again mass separated and studied with a γ -ray spectrometer. This, in conjunction with high resolution examinations of strong sources of chemically separated Praseodymium gave much new information about these isotopes and their cerium daughters and thus revealed an explanation of the apparent contradiction in the decay of Pr^{137} to Ce^{137} . The crux of the matter lies in the fact that the 254 kev γ -ray - previously ascribed to the ground state of Ce^{137} - actually is emitted by a long lived isomeric state, while Pr^{137} decays to a previously unknown ground state.

Thus Part A of this thesis describes experiments to improve the mass spectrometer while Part B presents the new results of investigations of Praseodymium and Cerium - particularly those of mass 137.

PART A: IMPROVEMENTS IN THE MASS SPECTROGRAPH

1. The Main Features of the Mass Spectrograph

The mass spectrograph in the McGill Radiation Laboratory has been described in detail by previous workers. (Dahlstrom 1953)(Maclure 1952) (See Fig. 1 and Fig. 2). Its outstanding feature is the use of 10 wartime magnetron magnets to provide the deflecting field. This greatly simplifies operation and removes the possibility of fluctuations in the field. On the other hand, the voltage on the ions is the only control on the mass selection.

The instrument was adapted from a design of Graham, Harkness, and Thode (1947) for a low cost mass spectrometer. It is a small Nier type sector instrument employing 90 degree deflection (Nier 1940). The analysing chamber is a 1.25 in. outside diameter copper tube 20 in. long, with 1/32 in. walls, and is bent on a mean radius of 6 inches. The section between the poles is flattened to 7/16 in. in depth. The copper source and collector chambers are approximately 4 in. in diameter and 4 in. in length. Brass plates press against 0-rings to seal off the two ends. By removing 4 bolts either chamber can be quickly opened for loading and unloading. The ion collector is insulated from the chamber and is connected to the preamplifier input.

The preamplifier and amplifier were constructed from the design given by Graham et al. (1947) and have a current sensitivity of 1 x 10⁻¹³ amps, per mm deflection on the galvanometer. This is more than adequate for use as a small separator, but it is extremely useful for quantitative monitoring of the ion current. If lines are swept across a fine exit slit, an accurate measure of the dispersion and resolution can be obtained.

The pole pieces are identical to those of Graham et al. with a 1/2 inch gap. They are bolted onto two soft iron yokes which extend by one gap width beyond the beam entrance and exit pole faces (see Fig. 2). For an ion which approaches and leaves the pole faces perpendicularly, the area of the yokes represents an idealized region of uniform magnetic induction, dropping off discontinuously to zero outside (Nier 1940) (Coggeshall 1947). This is a first order correction for the effect of the fringing fields. The apex, 0, for this type of instrument is approximately colinear with the defining slit and the plane of focus. The yokes rest on ball bearings, so that the magnet can be moved with respect to the fixed analysing tube. The magnets press firmly against the yokes (Fig. 1). The magnet field intensity is only 3400 gauss. This means the instrument must be used at unusually low accelerating potentials for heavier masses. For example, at about mass 150, the region of interest for Praseodymium studies, the accelerating voltage is only 600 volts. As a result, the ions must be nearly monoenergetic. The mass dispersion D between two adjacent isotopes of mass M and M + 1 is given by

$$D = \frac{R}{M}(a_{\bullet}m_{\bullet}u_{\bullet}) , \qquad (1)$$

where R is the radius of curvature. For this instrument, $D = \frac{152}{M}$ (mms.) Since

$$\frac{dV}{V} = -\frac{dM}{M} , \qquad (2)$$

the equivalent "voltage dispersion" between lines for M = 150, V = 600 volts, is only 4 volts.

The H.T. is provided by a commercial R.F. supply, variable from 500 to 2000 volts D.C., which can deliver up to 500 μ A. Electrical connections

can be made to the various ion source electrodes through kovar seals.

Rapid pumping down is provided by two three-stage oil diffusion pumps backed by a rotary forepump. Speed is needed, since with no vacuum locks, it is necessary to open the entire system to the air to load or unload the spectrograph. The system will pump to about 1×10^{-5} mm of Hg in 1/2 hour.

The main improvements made in the spectrograph include (i) resolution and in particular the contour of the mass lines were sharpened by empirical adjustment of the magnet relative to the analyser tube; (ii) radial focusing of ions with new lens system trebled the transmission; (iii) known masses are now collected on individual thin strips so that the selected radioactivity may be examined immediately upon the completion of the analysis.

The following sections describe the detailed experimental work which led to the above improvements.

2. The Characteristics of the Ion Source

The most important factor in the efficiency of a separator is the ion source, which converts the atoms or molecules of the sample into ions by some means, and then, with the associated lens system, projects as many as possible of the ions through the analyser.

The surface ionization source seems to be the only known ion source which can be used with the very low acceleration voltages permitted. It is monoenergetic except for the small voltage drop across the emitting portion of the filament. This is normally less than 0.5 volts. (The distribution due to thermal energies is a comparatively small effect.)

Richardson (1916) found that for thermionic emission, the positive ion current was similar to the electron current, and established an equation for its temperature dependence,

$$J = AT^{1/2} \exp^{-b/T},$$
 (3)

where J is the positive ion current density, T is the absolute temperature, and A and b are constants for the material. The positive ion current can result from the ions of the heated body itself; from an impurity in the body which can diffuse to the surface and be ionized; or from the ionization of a surface coating of certain substances.

Fowler (1936) derived a relation between positive ions and neutral atoms at the surface of a hot body. For a filament with a surface deposit, the efficiency of evaporation of the deposit as ions rather than as atoms or molecules is given approximately by the equation

$$\frac{n^{+}}{n^{O}} = \exp \frac{e(\emptyset - I)}{kT} \tag{4}$$

where n⁺ is the number of ions, n is the number of atoms or molecules, k is the Boltzmann constant, T is the absolute temperature, e is the electron charge, Ø is the work function at the evaporating surface, and I is the ionization potential of the evaporating deposit. This equation indicates that substances with ionization potentials less than the filament work function should be very good emitters, such as the alkali metals.

Blewett and Jones (1936) obtained currents from a number of salts of elements of higher ionization potential than the work functions of the filaments. Lewis and Hayden (1947), and Hayden (1947) obtained large currents from some of the rare earths evaporated on to the filament as nitrates, which decomposed to oxides upon heating. In general, for elements of valence 1 or 2 the ions were of the form X⁺, while for valence 3 or 4 the ions were of the form XO⁺. (X⁺ denotes the singly charged element ion, and XO⁺ the singly charged monoxide ion.)

Hayden (1947) measured the ionization efficiencies for many elements and compounds on a tungsten filament. The filament was mounted directly behind the defining slit of a mass spectrometer. The ratio of the current passing through the analyser to the collector over the current striking the defining slit disc was measured. This ratio was taken as the ion transmission efficiency (2%), and when multiplied by the ionization efficiency should equal the overall efficiency of the spectrometer. The latter was measured by integrating the total current at the collector from an aliquot containing a known number of atoms of the element in question. This integrated current is easily converted to the number of atoms collected, and the efficiency can then be determined. The efficiencies were reproducible to within 20%, provided samples of less than 100 $\mu \mathrm{gms}$. were used, and the temperature of the filament had been increased slowly. All values were taken with used filaments, since after repeated emission the efficiency increased by as much as a factor of two. The "memory" of a filament for the successive emission of the same element was less than 5%.

A portion of these values is reproduced here.

Ionization Efficiencies

TABLE I

Compound	Ion Type	Efficiency	$\frac{n^+}{n^0}$
La ₂ (NO ₃) ₃	LaO ⁺	16.0	
Ce ₂ (NO ₃) ₃	CeO ⁺	0.12	
$Pr_2(NO_3)_3$	Pro ⁺	12.0	
$Nd_2(NO_3)_3$	Nd ⁺ (1%) NdO ⁺ (9%) 1.0	

3. Investigations of Lens Systems

(a) The Potential Supplies. Both the H.T. load and the filament heating supplies were redesigned to provide better performance and more versatility. The H.T. load was altered to provide a variety of possible electrode voltage arrangements. (See Fig. 3). The elements of the load can be quickly rearranged into other sequences to provide any required accelerating voltage from 200 to 2000 volts. Terminal H is the filament H.T. supply; G and F are variable focusing supplies. I is connected to the repeller and provides a variable positive voltage of from 0 to 120 volts above the filament H.T. terminal.

This repeller circuit was added for reasons of stability. In the original circuit, the repeller voltage terminal was simply connected to the H.T. load. This proved very unsatisfactory at high filament temperatures, where the electron current to the repeller can become greater than 1×10^{-4} amps. This large current flowing through part of the H.T. load shifted the voltages on the electrodes by an amount dependent on the filament temperature.

The repeller supply was constructed completely separate from the H.T. load. It is encased in a lucite box for insulation. The l17 volt A.C. input is taken from a 60 V.A. Sola constant voltage transformer and applied through a 1 to 1 ratio isolation transformer to a selenium rectifier. The rectifier is rated for 130 ma. maximum current drain. The D.C. output is applied through a π filter to a 7.5 K. potentiometer. The negative side of the output is tied to the filament H.T. terminal and the centre tap is connected to the repeller. The regulation is adequate since the repeller voltage is an insensitive control on the focusing.

The filament heating supply was rebuilt completely (see Fig. 4). As shown in Fig. 4G, the forepump, diffusion pumps, and filament input supply were so connected that they can only be switched on in that order. This prevents a hot filament from being accidentally burned out by exposure to air. The normal filament supply is shown in Fig. 4A.

From the secondary of a high insulation transformer, 0 to 6.3 volts a.c. is applied to a 12 amp. full wave rectifier. The d.c. output is applied across the filament, which is centre tapped to the H.T. filament terminal. The ammeter A2 is normally connected across the shunt R3 and reads the filament current. When the microswitch S4 is held down, the meter reads the voltage directly across the filament. Since the filament resistance changes rapidly, an indication of power dissipation is necessary for good temperature control.

The duplicate supply (Fig. 4B) was made for use with a multiple filament to be described later. It is identical except for the output, where a double-pole double throw switch permits the heating of either one of two filaments. Both these filaments are centre tapped to the H.T. filament terminal.

(b) The Original Lens System. Previous workers had estimated the transmission efficiency of the spectrograph by measuring the quantity of current collected from a known sample and combining this with Hayden's values for the ionization efficiencies. Increasing the width of the defining slit increases the transmission but decreases the resolution.

Maclure (1952) gave a value of about 1%, using a 0.024 in wide defining slit. Since the dispersion is only 0.040 in. per mass unit in the mass 150 region, the defining slit must be kept narrow. Dahlstrom (1953) had found it necessary to use a 0.015 in. slit to resolve Praseodymium isotopes, and estimated the transmission efficiency as less than 1%.

A conventional type lens system had been used. Two horizontal deflecting plates F₁ and F₂ with a 1/8 in. separation were located 1/4 in. behind the grounded slit S. (See Fig. 2). The filament electrode was essentially the same as that shown in Fig. 5A, and was located 1/8 in. behind the deflecting plates. A d.c. voltage applied across the two halves heated the filament. A plane repeller R was situated 1/8 in. further behind. Four brass mounting rods, closely fitted with pyrex tubes, protruded from the front of the ion source chamber. The electrodes slid over these insulated tubes and were spaced with short lengths of larger pyrex tubing. The repeller and deflecting plates focused the ions on the slit. The repeller operates a few volts more positive than the filament. It collects the electron current emitted from the hot filament, while repelling the positive ions. The electrode potentials were tapped off from a chain of resistors and potentiometers between the H.T. supply and ground.

(c) The New Lens Components. Since the slit size cannot be increased, to improve the lens system more of the beam must be focused through it with small angles of divergence in both the horizontal and vertical planes. The magnetic field provides horizontal focusing but the line spread is proportional to the angle of divergence. The vertical divergence is much more important. The clearance in the analysing tube at the joint to the collector chamber is less than 5/16 in., and this is 20 in. from the slit. Thus a parallel beam is a necessity for high transmission. The standard lens system, such as the one described above, is a horizontally oriented cylindrical lens, and

provides no direct control in the vertical plane. It was decided to attempt to build a radial type of lens system, using discs with circular apertures, which would give complete focusing along the beam axis. It was hoped the ions would be focused to a small cross section and then be transmitted down the analysing tube as a parallel beam. A close approximation to this condition was realised (Sec. e).

The frame for the system consists initially of a 1/8 in. thick circular brass plate, 3 3/8 in. in diameter, with a 3/4 in. central hole (to let the beam through), and this plate is bolted rigidly into the front end of the ion source chamber (See Fig. 6). Four 1/8 in. brass rods, symmetrically spaced 1 1/4 in. apart, protrude from this plate back 3 1/2 in. into the chamber. The ends of these rods are threaded and a plane stainless steel disc with four similarly placed holes fits snugly over the rods. When machined teflon spacers suitable for the chosen lens components are slid into position, this back plate is brought up snugly against them with four brass nuts. This unit thus provides a solid source holder for mounting elements of a gun, and is long enough to permit a great variety of electrode arrangements. It should be noted that the machined teflon provided a more accurate alignment of lens components than could be realized with glass spacers.

All focusing elements are made from 3 3/8 in. diameter stainless steel discs, 0.030 in. thick. Each disc with a trial slit is fitted directly over the four metal rods. When pressed against the front plate, the slit is in the proper position, and is grounded through the frame (S, Fig. 6). All other electrodes have 3/16 in. holes which fit snugly onto the teflon spacer shoulders. The front of the following spacer fits over this shoulder and the electrode is thus held firmly in place (Fig. 7).

Elements used in experiments with the lens system will now be described, but the selection finally adopted appears later.

Several filament elements were constructed from semi-circular plates spaced 1/8 in. apart (Fig. 5A). The two halves were joined together by insulating mica strips. Thin steel inserts between two mica layers provide rigidity. The filament ribbon is spot welded under slight tension between two tungsten wires. The filament is heated by applying a voltage across the two halves.

A pair of semi-circular plates with a 1/8 in. spacing, exactly like the separate halves of the filament elements, were used as horizontal focusing plates. This is similar to the original focusing system.

A variety of discs were made with various sizes of central circular apertures. The aperture edges were rounded to minimize polarization. Circular discs with no apertures were also used to intercept the entire ion current.

The above elements were joined by nickel wire to brass press seals.

These can be pressed onto any of the kovar connectors, providing the potentials required.

One disc with a fixed 0.015 in. wide slit and another with a variable slit adjustable up to 1/16 in. wide were made. The slits were beveled to knife edges; hence the penetrating ions avoid a "tunnel", which can become polarized.

Cleanliness of all parts is essential to prevent disturbing charges from building up on films. The metal parts were periodically boiled in royalene or acetone. They were rubbed with very fine emery paper every time they were used. The teflon spacers were boiled in aqua regia and rinsed with distilled water.

- (d) Some Principles of Ion Optics. In the description of the lens systems certain principles of ion optics should be borne in mind:
- (i) The path of an ion in an electrostatic field is independent of its mass.
- (ii) The path of the ions depends only on the shape of the field, or the potential ratios. The absolute values do not affect the focusing.
- (iii) The final energy of the ions in the analyser is determined by the potential of the emitting filament only and is not altered by any focusing potentials.
- (iv) Space charge effects appear only for currents greater than about 1×10^{-8} amps. (See Spangenberg (1948) or Pierce (1954)).
- (e) The New Lens System. A radial grid lens was finally used and consisted of two discs with circular apertures for focusing (See Fig. 6). The first disc, next to the filament, will be called the grid. In front of the grid is the second disc, which is always at ground potential. A plane ion repeller is inserted behind the filament. By varying the grid potential and the spacings and aperture sizes of the two discs, the focal length of the grid lens can be varied. The beam normally converges to a "cross-over" and then diverges again, travelling out into the electrostatic field free region. The focusing was found to be quite insensitive to the position of the repeller so it was permanently located 1/8 in. behind the filament and its position will not be mentioned further.

Incidentally, an Einzel or unipotential lens was first tried. It consisted of three closely spaced discs with circular apertures.

The outer two were grounded and the inner one had a variable potential applied to it. This gives a converging lens of variable focal length. The purpose was to arrange the two lenses so that the Einzel would produce a parallel beam, whose cross section would be a reduced image of the source. (The source is that portion of the filament with the emitting deposit on it. This is usually about 0.25 in. high, and is 0.030 in. wide). By suitable adjustment of the parameters, all of the ion beam was projected through the source and into the analyser. However only 7% appeared at the collector. The focusing effects of fringing magnetic fields were assumed to have a detrimental effect on the low energy ions. (Herzog 1953). To advance further it seemed necessary to separate the two parameters.

If the ion beam could be controlled in a purely electrostatic system, then the problem of superimposing the magnetic field could be considered. However, because of the good results obtained with the grid lens alone, the double lens system was not considered further.

To study the properties of lens systems it is necessary to be able to follow the progress of the beam. The entire region traversed is at ground potential, except inside a lens. A plane disc is mounted to measure the current at any desired point on the path of the beam and is grounded essentially through its connection to the d.c. amplifier. Thus it will not alter the electrostatic conditions. Not only will the current at the position of the monitor be obtained, but by observing the ion stain produced on the electrode, the actual cross section of the beam at that position is visible. Unfortunately the current cannot be monitored in this way through the analysing tube. However by setting up the lens near the back of the ion source holder, the ion beam can be

studied over about the first two inches of its path. This is adequate to establish its cross section and angles of convergence or divergence. The final collector intercepts the beam leaving the analyser under conditions similar to those which exist when a plane collector intercepts it at the exit from the ion source chamber. Therefore the efficiency of transmission through the analysing tube is given by the ratio of these two currents.

As explained below the emission can be reset to a given value quite accurately. This is necessary since after a current measurement has been taken at any point, the machine must be shut down to move the collector to a new position. Both the filament and grid are now set to the arbitrary value of 200 volts positive. Then there is no attractive field on the ions in the forward direction. The repeller is effectively grounded by connecting it to the amplifier. The filament dissipation is adjusted until the ion current to the repeller is the desired value. For any particular filament loading (since the relative positions of the filament and repeller remain unchanged), this current will represent a constant fraction of the total emission. Then, leaving the emission dissipation untouched, the electrodes are connected back to their normal voltages. The emission varies with the electric field applied, and that is why it must always be set up at the same potential. Similarly the electric field gradient on the filament must be kept constant when efficiencies are being measured.

To measure the overall transmission efficiency, the lens is focused to give the maximum current to the final plate collector. This current and the electric field gradient on the filament are noted. Then a plane collecting disc is inserted in front of the filament. The same

total emission can be obtained by putting this collecting plate and the filament both at 200 volts positive, and setting up on the ion current to the repeller, as usual. Then the electrodes are hooked up in the normal manner, putting the same electric field gradient on the filament as in the first case. The current measured by the collecting plate in front of the filament will be equal to the total current emitted. It should be noted that in this case of direct collection in front of the filament, the collecting plate is itself in the electric field. However it will be shown in the following section that at the low values of electric field used, the current registered is the true ion current.

Indium ions were used throughout in the efficiency tests for two reasons.

- (i) Indium is a very efficient emitter. A 100 $\mu \mathrm{gm}$. loading on tungsten will emit measurable currents for hours.
- (ii) Even more important, Indium ions are produced at a sufficiently low temperature that there is no background from the filament. At the higher temperatures required for Praseodymium, for example, a large background current is emitted, presumably from light alkali metals diffusing to the surface. This is of no consequence when collecting heavy ions through the analyser. However there is no mass discrimination in the source region, and so the ion current from the deposit is masked by this background when collecting in the source chamber.

Tests showed that the grid lens alone, using two 1/4 in. aperture discs, would transmit about 50% of the beam to the final collector. This was without any defining slit, but showed that the lens made the beam nearly parallel. The 0.015 in. defining slit next replaced the

grounded aperture of the lens. After varying the grid aperture size and the spacings, the transmission was found to be an optimum with a 1/4 in. aperture grid situated 1/4 in. behind the defining slit and 1/8 in. in front of the filament. This became the standard grid lens and is illustrated in position in the holder by Fig. 6. Smaller grid apertures increased the transmission beyond the lens, because of the smaller beam cross section produced, but this was more than compensated by the losses to the grid itself, unless the deposit was limited to a small area. A normal deposit 1/4 to 5/16 in. in length on the filament produced no losses to the 1/4 in. aperture grid. This length is needed in practice to allow a certain leeway in loading the source on the filament.

A parallel plate deflector installed in the source holder in front on the standard lens was used to determine the optimum source holder alignment. Horizontal deflection showed a broad plateau of uniform transmission efficiency. The vertical alignment is quite critical. With the lens focused for optimum transmission, the beam was scanned vertically across the collector. From the geometry of the tube, and the deflection applied by the plates, it was found that the beam height would be about 2/3 in. at the collector, if not for the confining walls of the tube. Since the tube is 5/16 in., this would indicate about 65% transmission, where scattering is ignored.

The transmission efficiency measured for the standard grid lens system averages 15 to 18%. About 25% of the ions pass through the defining slit and 60% of these are transmitted through the analyser. This efficiency for the grid lens appears to be much better than the estimates of less than 1% for the horizontal deflecting plates system.

However these old estimates were too low, since they were calculated on the assumption that the ionization efficiency values of Hayden applied in the present case. This is not so and will be dealt with in the following section. Meantime, the efficiency of the old system has been directly determined. The exact alignment obtainable with the teflon spacers, however, improves the performance of all systems. The two deflecting plates are always at equal potentials for maximum transmission, showing the symmetry of the structure. The efficiency measured for it ranged from about 4 to 8%. There is more variation with individual loadings. Probably this is due to the lack of any vertical convergence, so that the length of the deposit will determine the efficiency directly.

4. Studies of the Surface Ionization Effect.

The ionization efficiencies given by Hayden (1947) combined with the measured transmission for ions, would indicate an overall efficiency of above 1% each for Praseodymium and Lanthanum. It was learned from the quantitites of separated activities, and from monitoring stable samples, that the efficiency is actually about a factor of ten lower. Since the transmission efficiency had been measured repeatedly, the discrepancy must be due to the ionization efficiency.

Several general factors affecting surface ionization were observed. Filaments are often strongly radioactive after they have ceased to emit atoms of an active deposit. This activity seems to decrease somewhat with age of filament, and implies diffusion of the sample into the filament. The material probably diffuses in until equilibrium is attained for the particular filament temperature. This would be in line with the fact that used filaments become better emitters. The

filament temperature must be increased very slowly, especially in the region where the sample is outgassing. If the sample is large, or is heated too violently, some of it flows down the filament to the lower end. These factors are important, especially when dealing with activity, where speed is a primary consideration. However they were all carefully taken care of in Hayden's experiments on ionization efficiency and these cannot explain the large discrepancies in ions produced.

Workers have generally applied Hayden's values to situations where they do not apply. Thus it was found that measuring the emission from a filament at fixed temperature directly to a plane collector gave an increase of current with increasing electric field gradient. Two possible effects could be at work here.

- (i) Multiplication. Most of the secondary electrons emitted from the collector bombarded with the positive ions are of quite low energy (Spangenberg 1948). In an electrostatic field free region, particularly with the fringing magnetic field present, the electrons will be largely recaptured by the collector and so the current registered should be essentially the impinging ion current. However, when the collector is negative, and the electric field is increased, electrons eventually escape from the collector and are drawn to the filament electrode. This will appear as an increase in ion current to the collector.
- (ii) Field Emission. Another possibility is that the increased electric field can actually extract more ions from the evaporating surface. Since the temperature, and hence the evaporation rate, is fixed, this would be a net gain in efficiency. A simple calculation (Spangenberg 1948) shows that for any voltage beyond a few volts, the current is strictly temperature limited for the small ion currents used. (This is further borne out by the fact that the current very rapidly increases

with small temperature increases). Thus the current increase observed under high fields is due to field emission rather than from any space charge extraction.

These ideas were tested in the following way. A plane collector was set up 1/8 in. in front of the filament electrode. The filament was heated to give a steady Indium ion current, and values of the current as a function of the applied field were taken. This was repeated several times and gave consistent results. The combined results are plotted as Curve A in Fig. 8. The horizontal lower line at 1200 volts per in. field gradient represents the field applied for Praseodymium separations in the spectrograph. The upper horizontal line at 25,400 volts per in. represents the much higher field strength used by Hayden for the experiments in which he established the relatively high ionization efficiency values.

Next a grounded electrode with a 1/16 in. wide slit replaced the plane collector. The collector was put behind the slit. This slit was large enough to pass the entire current. (This was proved by monitoring it.) At the same time it presents essentially the same field conditions to the filament as in the first case. The dependence of current on field strength was repeated, but this time the collector was in a field free region. The results are shown as Curve B, Fig. 8, which is the same as Curve A up to about 6000 volts per in. Above this value, presumably, multiplication influences the values in Curve A.

The background emission at higher temperatures from the filament was measured at 1200 volts per in. and 14,800 volts per in. electric field gradients. This was done under both conditions of collection. Curves C and D were sketched through these points. Curve B represents true

thermionic emission of positive ions from a surface deposit. Curve D represents thermionic emission from the filament. Curves A and C give the result of ion emission plus multiplication.

It was impossible to go above 14,800 volts per in. field without extensive modification of the apparatus. However the curves illustrate that there is an important field emission relationship involved, and that the ionization efficiencies for a low voltage machine are inherently low.

Thermionic field emission, or Schottky Effect, has been studied extensively and a relation

$$\frac{I_E}{I_O} = \exp_{\bullet} \frac{AE^{1/2}}{T} \tag{5}$$

derived (Spangenberg 1948); where I_E is the emitted current in the field, I_0 is the normal temperature limited current, A is a constant, E is the electric field gradient, and T the absolute temperature. If an equation of this form applies to emission of a surface deposit, the variation of current with electric field will be a function of the temperature. Currents emitted at low temperatures would presumably increase more with field than those emitted at higher temperatures. If this is true, for the rare earths the increase of current with field would be less than for Indium, which is a lower temperature emitter. In that case, the relation describing the increase would lie between the extremes of Curves B and D. In any event, it can be seen that the ionization efficiencies will be lower than the values generally assumed.

Apart from this field emission effect, the values of the ionization efficiencies were formerly estimated about twice their true values.

Hayden measured the transmission by comparing the current reaching the collector with that measured at the defining slit. Since the slit

electrode was in a field of 25,400 volts per in., the apparent current was almost certainly too large due to secondary electron emission. The ratio of secondaries to primaries for metals in this voltage range is very nearly unity (Spangenberg 1948). At this high electric field gradient the current at the slit electrode could well appear about twice too large. This would cause the transmission efficiency to be apparently one half its true value, and thus the estimated primary ionization efficiency would be about twice its true value. Of course the product of these two efficiencies, which is the actually measured overall efficiency, would not be altered. However, when applied to another machine of known transmission efficiency, the resultant yield will be lower than expected.

5. The Multiple Filament.

The useful range of application of the surface ionization source has been greatly extended by Inghram and Chupka (1953) by the use of multiple filaments. As is shown in Eqn. 4, the higher the temperature, the greater the ionization efficiency, (except in the few cases where the ionization potential is less than the filament work function. With the multiple filament, the sample is evaporated at the appropriate temperature from one filament and a portion of the gas evolved strikes a nearby much hotter ionization filament.

Preliminary tests were carried out on a multiple filament design modelled after that of Inghram and Chupka. An electrode disc was split into 4 sectors as illustrated in Fig. 5B. Then completely separate left and right sample filaments were constructed as shown. Using them in conjunction with a third simple filament such as is illustrated in Fig. 5A, a U-shaped trough was formed. This is illustrated in Fig. 5C.

The second filament voltage supply (Fig. 4B) was attached to the side filaments. All three filaments are centre tapped to the filament H.T. terminal. Either the left or right sample filament can be heated by a throw of the switch. The unheated sample filament will collect some of the atoms evolved from the heated deposit on the opposite filament. When emission is completed from the loaded filament, by switching over and heating the opposite one more ions should be produced.

Because of the high thermal dissipation, lavite spacers replaced the teflon for the multiple filament. After machining, they were slowly baked to 1000°C. This produced quite uniform spacers. They must be used with more care than teflon, since the thin shoulders are quite brittle.

Preliminary tests with $Ce_2(NO_3)_3$ deposits showed improved emission over the single filament. However the vacuum would have to be considerably improved, perhaps by using cold traps, before the full potential of the multiple filament could be realized. The hot back filament at present burns out quickly at the very high temperatures normally employed (about 2700° K).

6. The Resolution

Some early separations of active Praseodymium isotopes showed that the resolution was initially inadequate and that there were large overlaps of isotopes into their adjacent lower mass neighbours. Tests on the resolution were therefore undertaken. Stable Praseodymium was used for these tests. Not only is it in the mass region of interest, but it is a 100% isotope Pr¹⁴¹, so that only one line is produced. By variation of accelerating voltage, the PrO⁺ ions were scanned over a 0.010 in. exit slit in front of the collector. The 'line' was found to have a peak

followed by a broad tail on the lower mass side. The tail was indeed even longer with the former lens system, using deflecting plates.

The trouble was found to be in the relative placement of the magnetic field. Previous workers had placed the magnet at its calculated location. The apex 0 was colinear with the collecting plate and defining slit, and equidistant from each of them (See Fig. 2.) The resolution was improved by wrapping soft iron wire or permalloy strips about the external parts of the analyser to shield it from fringing fields.

Since, however, the magnet can be moved with respect to the fixed analyser, it was decided to remove all shielding and empirically study the resolution as the magnet was moved about. As illustrated in Fig. 1, iron wedges were inserted between the four inner magnets and the yokes to shift them farther from the analyser. The resolution was improved slightly. The magnetic field was measured in the analyser tube. Inside the pole gap, the field was found to be extremely uniform. However, the fringing fields are large. At the positions of the defining slit and the collector they are about 55 gauss. (See Fig. 9).

To follow through with further studies of resolution, a new type of collector was used. The collecting plate (Fig. 10A), slides snugly into a track in a frame. (Fig. 10C). This frame is fastened to the insulated amplifier input terminal. The collector and track may be rotated about the central vertical axis. In addition, to catch the focal plane, the track can be moved forwards or backwards in the collector chamber. A rectangular slotted plate (Fig. 10B) bolts into position above the collector, as illustrated. It is held 0.030 in. away from the collector by teflon spacers. The slotted region is 9/16 in. high,

so the ion beam may fall entirely through this slot over its entire width of one inch. Any slit arrangement may now be made by welding thin vertical strips over one of these slotted plates. Fig. 10D is an example, having 3 slits. This slotted front plate is connected to a ground point in the collector chamber by a wire and clip. The teflon is such a good insulator that the amplifier sensitivity is not affected by the grounded plate. Now only ions passing through the slits are monitored and a resolution curve for any slit can be measured by scanning the line across it. To find the total current, the line is shifted off the slotted plate until it strikes one of the wide ends of the collecting plate.

A multiple slit was installed at 45° to the axis of the collector chamber. This is the approximate plane of focus. The resolution was recorded as the magnet was moved with respect to the X and Y axes (Fig. 2). This was repeated for various positions of the collector along the axis of the chamber. From this data, optimum positions for permanent location of the magnet and the collector were arrived at. It was found that the focal depth is so great that the collector can be installed normally rather than at 45° to the axis. For Praseodymium, there is now no appreciable defocusing over a central region equivalent to ten or twelve mass units.

The analyser was cleaned to remove condensed oil and baked out under vacuum for several hours. Dielectric layers on the walls can become charged and cause the lines to broaden, particularly at the ends.

As a result of these steps, the resolution was considerably higher.

The tailing off on the inner side was largely removed. This tail is

actually due to line curvature. Flux leakage can result in slightly lower

field intensities in the centre region of the gap than at the pole faces. This causes the ions to be deflected more at top or bottom than in the median plane. Any nearby iron, such as shielding, can increase flux leakage and accentuate this curvature. The result appears as poor resolution when monitoring through a slit.

The grid lens, using a 0.015 in. defining slit, gave a line 100% of which passed through a 0.020 in. exit slit, and 80% through a 0.016 in. slit. (This was for a collected current of 1×10^{-9} amps and corresponds to about 1×10^{-8} amps emission current. Space charge spreading begins to appear at larger currents. This means that the line width for an ion of mass about 150 is one half the dispersion. The 15% efficiency figure for transmission could be increased by widening the slit, but the purity of separation of activities is more important than a slight gain in transmission.

The resolution of the grid lens was also measured using the 1/16 in. wide exit slit. This slit actually does not define the beam at all, and all of it passes through. The electrode merely serves to establish the electrostatic lens conditions by providing a surface at ground potential. About 50% of the ions reached the collector. The resolution was surprisingly good and there were no broad tails. The shape was the same as with the 0.015 in. defining slit, except that the line was about three times as wide. While the latter condition is unsatisfactory for analysis of heavy active isotopes, it may be used with lighter elements to secure higher efficiencies.

7. The Collector.

With small spectrographs used as separators for madioactive isotopes, the activity has commonly been collected on a photographic plate. This plate can be passed under a lead slit and counter arrangement to monitor the lines. An easier, but still crude way is to use successive contact exposures of the plate to X-ray film. The degree of blackening on the films gives a measure of the decay period.

Gransden (1951) replaced the photographic plate by a piece of dural or copper foil. In contrast to the photographic plate, this has the advantage that defocusing charges cannot build up on its surface. After the collecting foil is removed from the instrument, a piece of no-screen X-ray film is placed in contact with it for a time suitable to produce line images. Pin holes are pushed through the film and foil so that they can be exactly realigned later. After the film is developed and dried it is realigned on the foil and the line positions are marked. The foil is then cut up into thin strips for counting.

This method was used for much of the work discussed in Part B. However, it was found to have many disadvantages. It takes some time to complete the many steps required. There is also the possibility of contaminating the isotopes by mechanical smearing when making contact between the film and foil. The cutting up is difficult when the line dispersion is so close to absolute requirements.

A collector was therefore constructed which collects the isotopes on pre-cut dural strips, which can be taken out and counted immediately after the separation. A slotted front plate (Fig. 10B) has a series of vertical bars spot welded to it. At normal incidence the dispersion for Praseodymium is 0.040 in. The strips used were nichrome ribbon 0.016 in. × 0.001 in. in cross section and were separated by 0.024 in. (See Fig. 10E). Stretched tightly on the face of the back collector plate is a sheet of 0.001 in. dural foil, which is held by the two bars a-a and b-b shown in Fig. 10A. (The foil is marked on the back with dye so that the exposed side can be identified.) This foil has been

slitt. previously with a razor blade to leave 0.040 in. wide vertical strips in the region of collection. The bars on the front plate are so positioned that they are centered over the strip edges. Thus the centre 0.24 in. region of the strips is directly behind the transmitting slots. Since the bars are grounded, as the voltage is varied on the filament, the lines will be centered on the strips at positions of maximum transmission. The front plate is opaque beyond 5 mass units on the high mass side of the centre (See Fig. 10E). This ensures that the active isotopes will be collected in the central region of optimum focus. The acceleration voltage is varied until the stable line, which is the only one giving a detectable current, is falling into the desired slot with respect to the opaque end. Then the mass number of each strip is known. At the completion of the run, the active strips are clipped free at both ends, and are mounted for immediate counting with their mass number already established.

With this method, the stable line is constantly being monitored through a slit. Thus the lens grid can be set at optimum focus. When collecting "blind" onto a plate, which can only be monitored for total current, the optimum focus is assumed to be at optimum transmission. In practice, the optimum focus is considerably sharper. In addition, slight periodic positional drift can be compensated for by keeping the stable line centered for maximum transmission. The 40% opaque region between lines provides a margin of safety to eliminate slight overlaps.

The strips must still be very carefully cut, but now this is done in advance. A jig was constructed to put the bars on the front plate and to cut up the foil. (Fig. 11A). The front plate (Fig. 10B) bolts securely into the jig carriage, which moves along a track. The carriage

movement is controlled by a calibrated screw. A length of the nichrome ribbon is stretched and held securely in fixed clamps, so that it is flush with the plate and exactly normal to the long axis. It is spot welded in place, and the ends are trimmed off. The carriage is moved to the next position and the process is repeated.

To cut up the collecting strips, the plane collector plate is mounted in the jig carriage. The foil is stretched evenly over the collector surface. The clamps for holding the chrome ribbon are replaced by the adjustable slit shown in Fig. 11B. This slit has two thick jaws, one of which is fixed exactly normal to the long axis of the plate. These jaws press down lightly on the foil. A razor blade is inserted between the two jaws. The adjustable one is pressed against the blade and tightened. The blade can be moved along the slit axis, but no lateral motion is allowed. The blade is simply drawn over the foil to cut it for a length of about 3/4 inches. Then the carriage is moved a distance equal to the dispersion and the process repeated. In this manner, several collectors are pre-cut and stored ready for use. Fig. 11C shows the front plate mounted on a collector installed in the frame.

SUMMARY AND DISCUSSION

A lens system was constructed which employs several new features.

A radial lens replaced the usual horizontal focusing plates system.

This radial lens focuses the beam both in the vertical and in the horizontal plane. Thus some direct control is maintained on the vertical beam spread, which is otherwise an important limiting factor on the transmission efficiency. The transmission efficiency for the entire system as a result of the improvements was 15% with a 0.015 in. defining slit. The width of this slit is dictated by the mass dispersion.

Where the dispersion permits, the defining slit can be replaced by a wide 'virtual' slit which provides the required grounded plane for the lens without defining the beam. The transmission is then 50%, and the resolution is adequate for separating isotopes lighter than about mass 50.

The use of an independent circuit between the filament and repeller, to dissipate the thermionic electron current, eliminated slight shifting of the H.T. potentials as the filament temperature is changed. However, the replacement of the present small R.F. unit by a more stable H.T. supply would be desirable.

Machined teflon spacers provide exact alignment of the lens components. The resulting structural rigidity allowed the source mount alignment to be carefully adjusted - using horizontal and vertical beam deflection as a guide - until the transmission was a maximum.

Empirical adjustments of the magnet position were used in conjunction with a novel multiple exit slit to find the optimum resolution conditions. The uniformity of the magnetic field is attested to by the high resolution of the instrument: the line width is 0.020 in. for a 0.015 in. defining slit.

A new collector for radioactive isotopes was constructed. The stable carrier is constantly monitored through a slit. Thus control of both the focusing and the position of the isotopes is maintained throughout the separation. The active isotopes pass through other slits, spaced a distance equal to the dispersion arrant, and then impinge upon pre-cut strips of foil. At the end of separation, the foils are quickly removed and are ready for individual monitoring. Furthermore, the opaque region between each slit increases the purity of the isotopes.

The radioactive separations carried out after all these features were incorporated gave stronger yields of better separated isotopes.

The complex problem of ion source efficiency remains the limiting factor in achieving strong sources of separated isotopes. Preliminary tests were carried out on a multiple filament system. These tests showed that the vacuum system needs improvement to permit the operation of filaments at the high temperatures required. Heavier filament ribbon for the hot ionization filament would also increase filament life. It should be borne in mind that the multiple filament only improves markedly the relative ion emission of elements which, because of their low evaporation temperatures, are very poor emitters from a single filament. For an element which is already an efficient emitter from a single filament, the increased ionization efficiency for the gas striking the hot filament is compensated for by the geometrical losses due to gas escaping entirely. The multiple filament then is essentially limited to the very useful purpose of making many poor emitters become fair emitters.

The discrepancy between the low ionization efficiencies obtained here and the high efficiencies measured by Hayden led to some interesting

observations on the effect of electric fields on surface ionization. From these it appears that the ionization efficiency of low voltage machines is inherently low.

Unfortunately the experiments described were carried out just previous to the completion of this project, so that it was impossible to look further into the matter. Nevertheless the information given is sufficient to show the importance of high electric fields on the efficiency. It would be interesting to investigate, over a wide range of electric fields, the field emission characteristics of a number of elements which emit at widely different temperatures.

Since the ion currents are a form of temperature limited thermionic emission, it is to be expected that some field emission would be at work. However it appears from the limited data obtained, that this factor may be large for emission from a surface deposit. With evaporation of gas and ions taking place from presumably a molten semi-conducting layer it would not be too surprising if the electric field gradient effects the ionization at the surface to a greater extent than at the surface of a pure metal.

The possibility that field emission could be utilized to achieve larger currents seems well worth considering. One obvious possibility would be to place a highly negative extracting electrode directly in front of the filament, to provide a very strong extracting field. This would be followed by a de-accelerating and focusing lens system. If such a system were made workable, the extracting field could be controlled independent of the actual positive filament voltage required for a given mass. Then the field emission effect could be exploited to its full advantage.

BIBLIOGRAPHY. PART A

- Blewett J.P. and Jones E.J., 1936. Phys. Rev. 50, 464.
- Coggeshall, N.D. 1947. J. Appl. Phys. 18, 855.
- Dahlstrom, C.E. 1953. "Neutron Deficient Isotopes of Praseodymium", (Ph.D. Thesis. McGill University)
- Fowler, 1936. "Statistical Mechanics", Cambridge University Press (Second Ed.)
- Graham, R.L., Harkness, A.L., and Thode, H.G. 1947. J. Scient. Inst. 24, 119.
- Gransden, M.M. 1951. "Properties of New Neutron Deficient Isotopes of Lanthamum", (Ph.D. Thesis. McGill University).
- Handley, T.H. and Olson, E.L. 1954. Phys. Rev. 96, 1003.
- Hayden, R.J. 1947. MDDC-1546.
- Herzog, 1953. "Mass Spectroscopy in Physics Research", U.S. Dept.of Commerce. Natl. Bur. Stnds., Circular 522, p. 85.
- Inghram, M.G. and Chupka, W.A. 1953. Rev. Sci. Inst. 24, 518.
- Lewis, L.G. and Hayden, R.J. 1947. IDDC-1556.
- Maclure, K.C. 1952. "Properties of Some Neutron Deficient Isotopes of Strontium, Indium, and Gallium". (Ph.D. Thesis. McGill University.)
- Nier, A.O. 1940. Rev. Sci. Inst. 11, 212.
- Pierce, J.R. 1954. "Theory and Design of Electron Beams". Van Nostrand.
- Richardson, O.W. 1916. "The Emission of Electricity from Hot Bodies", Longmans, Green, and Co.
- Spangenberg, K.R. 1948. "Vacuum Tubes", McGraw-Hill.

PART B

A DETAILED STUDY OF ISOTOPES OF PRASEODYMIUM AND CERIUM OF MASS 137.

I. A Survey of Previous Work.

Some information available at the beginning of this project on the isotopes in the region under discussion is given in Table I.

TABLE I

Data on Half-Lives and Percentage Abundances of Isotopes.

<u>Mass</u>	Praseodymium	Cerium	Lanthanum
142 141 140 139	19.2 hr 100% 3.5m 4.5 hr	11.1% 32 d 88.8% 140 d	74m 36 hr 40 hr 99•91%
138 137 136 135 134	2.0 hr 1.5 hr 1.1 hr 22 m	0.25% 36 hr 0.19% 22 hr 72 hr	2 x 1011 yr 400 yr 9.5 m 19 hr 6.3 m

Stover (1951) studied neutron deficient praseodymium activities produced by proton bombardment of cerium metal. At 10 Mev, (p,n) reactions gave the previously known 19.5 hr Pr¹⁴² and 3.5 min. Pr¹⁴⁰ (Dewire et al. 1942). At 20 Mev a 4.5 hr activity appeared which was shown to be the parent of 140 d. Ce¹³⁹. This isotope, Pr¹³⁹, decayed partly by positron emission, with a maximum energy of 1.0 Mev. The K-capture to positron ratio was 1: 0.06. At 32 Mev a 2.0 hr activity appeared and was assigned to Pr¹³⁸. A 220 kev conversion electron was associated with it, as well as 160 and 1300 kev γ-rays. The positron maximum energy was given as 1.4 Mev, and the K-capture to positron ratio as 100:13.

Dahlstrom (1953) bombarded cerium oxide at various energies with protons and mass separated the resultant activities. These confirmed

the 4.5 hr Pr^{139} and 2.0 hr Pr^{138} assignments. A new isotope appeared at mass 137 with a 1.5 \pm 0.1 hr half-life. Its positron end point energy was 1.8 \pm 0.1 MeV, as measured with a long-lens β -ray spectrometer. No activity was observed at mass 136. The γ -rays of 300, 800, and 1050 keV observed showed a half-life assigning them to Pr^{138} . The strong 300 keV transition gave strong K- and L-conversion electrons in the ratio of about 3:1.

Handley and Olson (1954) bombarded both natural cerium and cerium enriched in isotopes Ce^{136} and Ce^{138} with protons at various energies. They studied the γ -ray spectra and the positron maximum energies of the resultant activities. For Pr^{139} they found γ -rays at 170, 1300, and 1600 kev, in addition to X-rays and positrons. The maximum energy of the positron was measured as 1.0 \pm 0.1 Mev. The 2.0 hr Pr^{138} gave a positron maximum energy of 1.4 \pm 0.1 Mev. Both these end point energies agreed with the results of the previous workers. γ -rays at 300, 800, and 1050 kev were observed in Pr^{138} , agreeing with the findings of Dahlstrom.

However, no activity was found due to Pr^{137} . In addition the Ce^{137} daughter of Pr^{137} was searched for without success. The 250 kev γ -ray characteristic of 36 hr Ce^{137} was not present. It was calculated that the half-life of Pr^{137} must be less than 5 min. or greater than 1 yr.

A new 70 min. activity was assigned to Pr^{136} , on the basis of yields, with γ -rays of 170, 800, and 1100 kev energy. Its maximum positron energy was given as 2.0 \pm 0.1 Mev. An additional activity of 22 min. was assigned to Pr^{135} . γ -rays of 80, 220, and 300 kev energy were found. Its positron maximum energy was measured to be 2.5 \pm 0.1 Mev.

For Ce¹³⁷, Inghram and Hess (1948), using a mass separator, assigned a half-life of less than 2 weeks. The upper limit for La¹³⁷ was set at 30 yr. Chubbuck and Perlman (1948) gave a half-life of 36 hr to Ce¹³⁷.

No positrons were observed, but a 280 kev γ-ray was detected. The upper limit for the half-life of La¹³⁷ was raised to 400 yr. Stover (1951) agreed with the 36 hr assignment, although the energy of the γ-ray was placed at 240 kev. Hill (1951) again agreed with the previous workers but changed the energy of the transition to 257 kev. Keller and Cork (1951) obtained a 180 degree beta-ray spectrograph plate showing three conversion electron lines. These were fitted to a 253.4 kev transition in La¹³⁷, following electron capture from 36 hr Ce¹³⁷. The K- to L-conversion ratio was estimated as about 10:1.

II. The Irradiations and Chemical Separations.

(a) The Targets

Both cerium oxide and cerium metal were used as targets for the production of praseodymium isotopes. About 20 milligrams of the powder was packed into a 1/8 in. diameter tube about 1/4 in. long, made from 0.0006 in. Al. foil. This tube was mounted in a dural clamp. When the metal was used, a flattened piece was mounted uncovered directly in one of the dural clamps. It was stored in C Cl₄ until the time of bombardment, to prevent oxidation.

The cerium oxide was prepared by igniting ammonium hexanitrate cerate (G.F. Smith Chemical Co. Reference Purity) to about 250° C. The lanthanum oxide was Johnson and Matthey Spectroscopic Grade lot no. 6781. High purity lanthanum and cerium metals were obtained from the Ames Laboratory through Dr. F.H. Spedding.

The dural block/clamped onto the water cooled internal probe of the McGill 82 in. synchro-cyclotron. The proton beam used on the metal was about one microamp. The cerium oxide powder had to be bombarded at reduced beam intensity, since at high temperatures it changes into a form which is hard to dissolve. After bombardment, the tube was torn open and the powder poured out. When the metal was used, only about the front 1/16 in. protruding into the beam was cut off and chemically separated.

The lanthanum targets were prepared in the same manner as the cerium targets. They were bombarded at about one microamp. proton current.

All the spectroscopically pure target materials contain less than 1×10^{-4} parts of any other rare earths. The times of bombardment varied from about two minutes to 4 hours, depending on the half-lives involved and the type of source prepared.

(b) The Chemical Separations.

The chemical separation of the rare earths is normally very difficult because of the similar electron configurations. Ion exchange columns are usually used, but are rather slow, if pure separations are required. Fortunately cerium can be oxidized to a +4 valence state under conditions in which lanthanum and praseodymium will remain in the normal +3 valence state. This fact is the basis of the separations used.

(i) Lanthanum Targets

The La metal or oxide, contained in a 15 ml. centrifuge tube, is dissolved in 1 ml. of concentrated nitric acid and is then cooled in an ice bath.

About 10 mgms of solid potassium bromate (KBrO₃) are dissolved in the solution to oxidize the cerium to its +4 valence. Then 300 micrograms of zirconium (Zr) carrier are added. The addition of 2 mls of saturated potassium iodate (KIO₃) precipitates both the Ce and the Zr. The solution is centrifuged, and the supernatant containing most of the La target removed.

Three mls of a solution containing 1 part HNO3 and two parts KIO3 are added to the precipitate, plus a little more KBrO3 to ensure continued oxidation. This solution is stirred and re-centrifuged. The supernatant contains some more of the La target. Several of these purification cycles are carried out until La is entirely removed. To test the supernatant for La, ammonium hydroxide is added. An <u>immediate</u> white precipitate indicates that La is still present.

Now the Ce must be reduced to the +3 valence to permit its removal from the Zr carrier. The precipitate, which contains both the Ce and Zr, is dissolved in a few drops of conc. HNO3. Three drops of H_2O_2 are added to reduce the Ce. The addition of 1 ml. of KIO_3 again precipitates the Zr, but the +3 Ce remains in the supernatant. Two of these extraction cycles remove almost all the Ce.

One half milligram of iron carrier is added to the combined supernatants containing the Ce. This solution is rendered basic with NH4OH and the iron precipitate carries the very small cerium hydroxide precipitate with it. The precipitate is washed twice with water to remove salts. It is then dissolved in a minimum volume of 6N HCl. The iron is removed with about three ethyl ether extractions. The HCl containing the activity is boiled down to one drop, ready for preparing

The ether extraction is very efficient, and practically no losses of activity occur.

Since the cerium half-lives were quite long the chemistry was done very carefully over a period of about 2 hours, repeating such steps as proved necessary. As a result, about 85% of the cerium activity was extracted. This was carrier free except for the small amount of stable cerium present in the target.

(ii) Cerium Targets

The early praseodymium separations were carried out using a method in which the valence +4 cerium was precipitated as a phosphate.

(Dahlstrom 1953). However, after the development of the iodate separation for La targets this was also adopted for Pr, since the conditions seemed less critical for the iodate than for the phosphate precipitation.

The procedure is essentially the same as for La, since La and Pr behave similarly with respect to Ce. However, in this Pr separation it is the cerium target material rather than the produced activity that is initially precipitated. This means the volumes dealt with are larger. For that reason the Ce targets are kept as small as possible.

A complication arises in that the oxide and the metal are both insoluble in conc. HNO3. When the oxide is used, it is dissolved by heating in a beaker containing 1 ml. of HNO3 plus 1 ml. of $\rm H_2O_2$. After the powder is dissolved, the solution must be boiled down until all $\rm H_2O_2$ is removed, since this is a reducing agent.

When cerium metal is used, it is dissolved in a beaker containing 1 ml. of hot HCl. Then 1 ml. of HNO3 is added and the solution boiled down to a small volume. Again HNO3 is added and the solution is once more boiled down to a small volume. These steps replace the HCl with HNO3.

The separation can now go forward for either the metal or the powder.

Two mls. of HNO3 are added and the solution cooled in an ice bath. About 50 mgms. of KBrO3 are dissolved in the solution to oxidize the cerium.

About 10 mls. of saturated KIO3 precipitates the Ce target. The solution is centrifuged in a 50 ml. centrifuge tube, the active Pr remaining mostly in the supernatant.

The supernatant is transferred to a 15 ml. centrifuge tube. About 500 micrograms of Zr carrier are added, plus a little more KBrO3 and KIO3, and the solution is again centrifuged. This step removes any Ce that may not have precipitated the first time. The supernatant contains the Pr activity in an iodate solution.

At this point, Pr can be freed from the solution in exactly the same manner that was used for Ce. Iron carrier and NH₄OH will precipitate the Pr. This is followed by washing with water and ether extraction of the iron. The HCl solution containing the Pr can be boiled down to a drop, ready for making either γ - or β -ray spectrometer sources.

However, for mass spectrograph use, the Pr must be applied as a nitrate. This requires boiling the 6N.HCl solution to dryness, followed by the redissolving of the activity in a drop of HNO3. The ether extraction, boiling dry, and redissolving, takes some time. In addition, a good part of the activity adheres to the glass.

A simpler extraction was found for the preparation of mass separation sources. The iodate solution containing the activity is rendered basic with NH4OH, without the addition of any other carrier. The ammonium iodate separates out and itself serves to carry down the activity. There are always a few micrograms of rare earth impurities remaining which also precipitate. After centrifuging, the activity and impurity stick to the walls and the iodate salts can be carefully removed with about two water washings. Then the activity is dissolved in a few drops of HNO3, and is again precipitated with NH4OH, to ensure complete removal of salts. The small precipitate of impurities carrying the activity is barely discernable as a thin film in the tip of the centrifuge tube. After washing, it is dissolved in one drop of HNO3, and can be loaded on the filament.

This extraction is considerably faster than the iron procedure. Since the amount of precipitate is small, the losses in washing are large. However, the Pr half-lives are short and efficiency of recovery must be balanced against speed in the chemistry. The recovery of activity is about 50% in the overall Pr separation.

III. Source Preparations

To prepare a source for the mass spectrograph the filament electrode was placed horizontally beneath a heat lamp. When the filament was quite hot, the activity, contained in a drop of nitric acid, was carefully applied with a micro pipette to the central region. This dried quickly and was then installed in the spectrograph.

For the NaI(T1) spectrometers, the activity, in a drop of acid, was applied to the surface of thin teflon cloth or scotch tape. The drop was dried and then a layer of scotch tape was applied over the surface.

The sources for the long-lens β -ray spectrometer were mounted on thin film (approximately 20 micrograms per cm²), made from V.Y.N.S. Resin obtained from the Department of Radio-Chemistry at McGill. These were very lightly gold plated to ensure electrical grounding for the source. The spot size was defined by a drop of insulin. This was washed off with water and then the activity was applied to the spot. Very gentle drying was required. On occasions where speed was essential, the activity, contained in a drop of nitric acid, was simply dried on a thin piece of niobium foil.

Preparing 180° β -ray spectrometer sources presented the most difficulty. Here the source activity must be applied to the surface of a thin wire, preferably as small as 0.002 in. in diameter. The usual method, for suitable elements, is electro-chemical deposition, in which the wire is made one of the electrodes in a solution of the activity. The conditions required vary with the element and the efficiency is normally low.

A simple and fast "physical" method was developed which would apply equally well to other elements. It is based on the preferential "wetting" of the wire compared with certain other materials. If a wire is laid in the bottom of a wax trough and a drop of solution applied, the solute will dry preferentially on the metal surface. This was tried but wax was abandoned, since it tends to coat the wire surface and, furthermore, it cannot be heated to speed drying.

Teflon was found to have the desired properties. It is non-wetting, inert to HCl or HNO3, and is stable up to high temperatures. A trough was cut across a 1/2 in. wide piece of teflon, using a 30 degree milling tool, to a depth of 1/8 in. Then, a fast rotating cutter blade made a

smooth sharp angled cut a few thousands of an inch deeper in the bottom of this trough. A 0.002 in. wire fits snugly into this finer trough. The larger trough provides the holding capacity.

A tantalum wire is fixed in the source holder of the instrument and is cleaned with acid. The teflon block, after being thoroughly cleaned, is mounted in an adjustable clamp. It is then screwed into position with the trough tight up against the wire. The drop containing the activity is pipetted into the centre of the trough. Because of the non-wetting of the teflon, surface tension holds the drop at the centre. It is heated to dryness under a heat lamp. The source holder can then be installed immediately in the spectrograph.

About 1/3 of the activity remains on the wire surface, confined to a short region.

IV. Studies on Praseodymium Isotopes in the Mass 137 Region.

- (a) The Mass Separations
 - (1) Separations and Detections

The isotope Pr¹³⁷ was re-investigated with the mass spectrograph and the contradictory evidence was resolved. Since the Ce¹⁴⁰(p,4n)Pr¹³⁷ cross section should peak in the vicinity of 40 MeV, irradiations were carried out at proton energies ranging from 30 to 55 MeV.

Fortunately, praseodymium is about 100 times as efficient an ion emitter as cerium. Thus the separated activity of given mass number is essentially all emitted from the filament as $Pr0^+$. This makes the analysis of the decay of the parent to its cerium daughter much simpler than if significant amounts of cerium activities were themselves emitted.

The cerium target, although spectroscopically pure, contains a few micrograms of other rare earths. These small quantities in part survive the chemical separation and are loaded on the filament with the activity. The ion current produced from these stable components, which is practically all from Pr^{141} and La^{139} , is essential to the monitoring of the mass separation, (since the minute amounts of activity produce no perceptible ion current). Unfortunately, even the small quantities involved are more than sufficient, emitting a current of 1×10^{-8} amps. for about one hour. This fact, plus the variety of other time consuming factors involved, means that half-lives much shorter than one hour will not survive the separation in sufficient quantities to give significant counting rates.

The γ-ray spectra of the separated isotopes were studied with a 28 channel pulse height analyser designed by Dr. R.E. Bell. (Skarsgard 1954). This instrument was ideal for the rapid recording of a maximum of information obtained from the separated components in the limited time permitted by their short half-lives.

The detector used employed a l in. x 1.5 in. NaI(T1) crystal, in contact with a Dumont 6292 photomultiplier tube. To keep the background low, the detector unit was installed in a lead castle lined with iron.

The multi-channel analyser or "kicksorter" sorts and integrates the pulses of the energy spectrum, while simultaneously displaying the output on an oscilloscope. After adequate counts are taken for the required statistics, the counting is stopped and the γ -ray spectrum is recorded by an Esterline-Angus recorder. The time at which the count took place, and the time increment during which counts were integrated, are also recorded. Thus the counting rate at the particular time for the various γ -rays can be easily calculated.

For one standard detector, the absolute counting rate for a γ -ray is known as a function of its energy, for certain fixed distances from the crystal (Skarsgard 1955). The counting rate 'N' in the photoelectric peak is divided by an efficiency factor 'S' to give the absolute counting rate. Thus, in addition to obtaining the half-lives, the absolute intensities of the gamma rays (including the X-rays and annihilation radiation) can be determined.

Each separated active foil was mounted between two layers of scotch tape, which were stretched over a lucite ring. To count an isotope, it was set directly on the thin aluminum cover of the crystal. When annihilation radiation was counted, a 1/4 in. thick aluminum disc was placed on the foil, sandwiching it between the disc and the cover of the crystal to ensure complete annihilation. The annihilation rate (which is twice the positron counting rate), as well as the various γ -rays and X-ray rates, was recorded for each active isotope.

It is normally a bad practice to count an activity placed close to the crystal detector. Anomalies can appear in the efficiency versus energy relationship that are not present at larger distances. In addition, the annihilation of positrons directly against the crystal cover may permit some to penetrate into the crystal before annihilating, which can produce pulses of other than 511 kev.

In spite of this difficulty in obtaining absolute rates, counting at small distances was necessary for these weak and short lived activities. In any case, the direct identification of the half-lives of the isotopes and their daughters was the purpose of the mass separation. Once the half-lives and characteristic γ -rays have been assigned, strong unseparated sources can give further quantitative information.

However, the X-rays and positrons are common to all the isotopes, and thus the K-capture to positron branching ratios can only be properly measured for the mass separated activities. For this reason the relative efficiencies for 33 kev K X-rays and for annihilation radiation were measured both at 3 cms and at the position used for the separated isotopes. A Ce¹³⁹ standard provided the X-rays, and a Na²² standard, the annihilation radiation. Since the absolute efficiencies are known at 3 cms (Skarsgard 1955), the efficiencies were calculated for the conditions used in the experiments.

In addition to the "kicksorter" spectrum analysis, another detector and single channel pulse height analyser were used simultaneously. The channel window was set on the 33 kev X-ray peak characteristic of the elements involved. The width of the "window" was such that slight drifting would not affect the counting of the whole peak, but still kept the background count very low. The various isotopes were monitored in rapid rotation for X-ray counting rates, so that good decay curves were obtained. This information supplemented the energy spectrum analysis given by the "kicksorter".

(2) The Results

Irradiations at 45 to 55 Mev produced consistently four strong activities, at mass 139, 138, 137, and 136. Short exposures of X-ray film to the collecting foil immediately after mass separation showed four lines at the positions of these masses. After a 55 Mev bombardment and mass separation on a copper foil, a contact X-ray film exposure of several days duration, commencing twelve hours after separation, showed lines at mass 139, 137, 135, and 134.

While the decay of Pr137 was the problem which was primarily studied,

the information obtained on Pr¹³⁹, Pr¹³⁸, Pr¹³⁶, and the lighter masses during the course of this study will also be presented.

Pr 137

The existence of 1.5 hr Pr^{137} was confirmed. (Dahlstrom 1953). The decay of the 511 kev annihilation radiation consistently gave the 1.5 \pm 0.1 hr value for the half-life.

However, the decay of the X-rays gave 1.5 \pm 0.1 hr, growing into 9.0 \pm 1 hr. (See Fig. 12). Evidently the 1.5 hr transition goes to a previously undetected state which decays by electron capture, with a 9 hr half-life. A very weak 440 kev γ -ray appeared in the spectrum, after the 1.5 hr annihilation radiation had decayed to insignificance. No activity which could be attributed to 36 hr Ce¹³⁷ was found.

The 1.5 hr decay exhibited no γ -rays of detectable intensity. Fig. 13a shows the Pr¹³⁷ spectrum in the region from 0 to 1 Mev. An upper limit of about 10% of the annihilation intensity can be set on undetected γ -rays. For high energy transitions, peaks smaller than this limit could probably be detected, but at low energies backscatter and general background radiation make the detection of weak γ -rays difficult. (The upper limits quoted on unobserved γ -rays throughout this work are for the uncorrected photoelectric peaks.) Fig. 13b shows a background count for the energy range 0 - 1 Mev.

The K X-ray to positron ratio was calculated approximately by comparing the intensities of the 33 kev and the 511 kev peaks. In arriving at this estimate, corrections were made for the X-ray intensity from the 9 hr daughter as well as the general background.

The branching ratio is given by

$$f = \frac{\lambda_K}{\lambda_+} = \frac{\frac{\lambda_K}{N_+}}{\frac{N_+}{N_+}} \tag{1}$$

where N_{K} is the intensity in the K X-ray peak

 N_{+} is the intensity in the annihilation peak, divided by two

 ω_{K} is the fluorescent yield for K X-rays of 33 keV

 $\delta_{\mbox{\scriptsize K}}$ is the counting efficiency for the K X-rays

and δ_{+} is the counting efficiency for 511 kev γ -rays.

The K X-ray correction results from competition from K-Auger electrons. The K-fluorescent yield is defined as:

$$\omega_{K} = \frac{X_{K}}{V_{K}} = \frac{X_{K}}{A_{K} + X_{K}} \tag{2}$$

where XK is the number of K vacancies resulting in K X-rays,

 ${\tt A}_{\rm K}$ is the number of K vacancies resulting in K-Auger electrons,

 $V_{\mbox{\scriptsize K}}$ is the primary number of K shell vacancies.

A plot of experimental values of ω_{K} as a function of the atomic number Z is given by Bergstrom (1955), (as reproduced in Siegbahn 1955), For cerium (Z = 58), or praseodymium (Z = 59), the value is ω_{K} = 0.88.

Of course, λ_K and λ_+ are the decay constants for K-capture and for positron emission, and are directly proportional to their respective disintegration rates.

The ratio of the efficiencies, as measured directly on the crystal cover, was

$$\frac{\delta_{+}}{\delta_{K}} = \frac{0.107}{0.287} = 0.373.$$

Average experimental values were $N_K = 14.0 \pm 1$ cps., and $N_+ = \frac{1}{2}(5.8\pm1)$ cps. This gives $f = 2.05 \pm 0.2 \text{ for } Pr^{137}.$

Pr139

The spectrum of 4.5 \pm 0.1 hr Pr¹³⁹ was also studied. No γ -rays were found of intensity greater than 5% of the annihilation peak, with the exception of a possible transition of about 3% of the annihilation intensity at 1150 kev. This is shown in Fig. 14a and, although small, it appeared consistently. The 140 d. Ce¹³⁹ γ -ray of 166 kev energy became weakly evident after the 4.5 hr parent had largely decayed.

The ratio of K-capture to positron emission was

$$f = 11.3 \pm 1.0$$

Pr138

Pr¹³⁸ displayed a large number of γ -rays, in addition to the annihilation radiation and X-rays. The half-life was 2.1 \pm 0.1 hr; decaying to a stable daughter, Ce¹³⁸. Intense γ -rays were observed at 300 \pm 10, 800 \pm 10, and 1040 \pm 10 kev. (Fig. 15b). Less intense peaks also appeared at 1295 \pm 15 and 1590 \pm 20 kev. Any still higher energy γ -rays are less than 10% of the intensity of the 1590 kev transition.

A 160 kev γ -ray was also tentatively assigned (Fig. 15a). The K X-ray to positron ratio was

$$f = 4.5 \pm 1.2.$$

It should be noted that the K X-ray intensities include contributions from K-conversion electrons. However, it will be shown in the following section that the only intense conversion electrons are due to the 300 kev transition in Pr¹³⁸. Thus its measured apparent branching ratio will be somewhat high due to this contribution.

Pr136

A praseodymium isotope of 1.0 ± 0.15 hr half-life was found at mass 136. Its annihilation radiation and K X-rays both showed this

period, indicating decay to stable Ce¹³⁶.

Because of its short half-life, it was not obtained in as large quantities as the longer lived components, and, as a result, its half-life, which fitted 1.0 hr on several occasions, cannot be definitely given to better than 15% accuracy. Fig. 16 shows a typical decay curve. Because of the lower intensity obtained, the general background radiation plays a more significant role than with the other isotopes. This background is due to scattering and slight contamination from adjacent long lived components.

However, this result provides a definite assignment to Pr^{136} , confirming the previous results of Handley et al (1954) obtained on the basis of relative yields.

The K-capture to positron ratio was measured as

$$f = 1.8 \pm 0.4$$

No γ -rays were observed, and an upper limit of 10% of the annihilation intensity can be put on any that may be present. (Fig. 14b).

Lighter Isotopes

While no attempt was made to produce lighter isotopes by bombarding at higher proton energies, still at 50 and 55 Mev there was evidence for some activity.

At mass 135 no short lived decay was observed, which indicates that Pr^{135} has a half-life considerably less than 1 hour unless, as seems improbable, it is long lived.

The half-life of the activity observed was roughly 20 hours. Both Ce^{135} (22 hr) and La^{135} (19 hr), or some combination, are compatable

with this within the accuracy of the result. However the yield was too great to be attributed to direct emission of Ce¹³⁵ ions from the filament, because of the low ionization efficiency of cerium. Because of the high purity of the target cerium, the quantity of La¹³⁵ produced directly from other than (p,2pxn) reactions will be negligible. Furthermore, the quantity of La¹³⁵ produced by the decay of Ce¹³⁵ during the process will not be large. At 50 MeV, the Ce¹⁴⁰ (p,2p4n) La¹³⁵ cross section will be small compared with the (p,6n) cross section.

The only consistent interpretation is that Pr¹³⁵ is sufficiently long lived to partially survive the chemistry and mass separation, so that some Pr¹³⁵ is emitted from the filament. Since the time lapse from the beginning of emission of ions until the start of counting was of the order of 1.5 hours, a short lived isotope would have time to decay to insignificance. This is consistent with the Handley et al assignment of 22 minutes to Pr¹³⁵.

At 55 Mev a weak activity appeared at mass 134 with a half-life considerably longer than that observed at mass 135. The yield was small and all that could be concluded was that this is consistent with the assignment of a 72 hour half-life to Ce¹³⁴. (Hollander et al 1953).

b) The Conversion Electron Spectrum

Cerium was bombarded with 50 Mev protons and the resulting praseodymium activity was separated chemically. The conversion electron spectrum was studied in a thin-lens 3-ray spectrometer of 2.1% resolution and 1.4% transmission.

The spectrum revealed a large positron background and an Auger electron peak, both of which gave a composite decay.

Only the K- and L- conversion lines of a single transition were prominent (Fig. 17). Its energy was measured as 300 ± 5 kev. The half-life is 2.1 ± 0.05 hr, followed to zero intensity. The $\frac{K}{L+M+}$ ratio was 2.2 ± 0.1 . Weak K-conversion lines due to 800 ± 7 and 160 ± 2 kev transitions also were present with a 2.1 hour half-life. Their intensities were small, but they maintained a constant porportion of the 300 kev conversion lines during the decay, and as a result can be assigned to Pr^{138} .

The 160 kev energy was found quite accurately by comparison with the known 166 kev Ce¹³⁹ transition (See Fig. 17). As the 2.1 hour activity decays, the 166 kev conversion line, being 140 days, comes increasingly into the picture until finally it alone remains.

The intensities of the K-conversion lines at 800 and 160 kev are both about 3% to 5% of the 300 kev K-conversion line.

Weak long lived peaks eventually appeared due to 255 \pm 5 and 280 \pm 5 kev transition K-conversion lines.

A weak conversion due to a 440 \pm 5 kev transition was also evident, with about a 10 hour half-life.

(c) Conclusions and Analysis of Results

The many new facts disclosed in this study of certain light isotopes of presendymine has not only corrected earlier interpretations of a relatively minor nature, but, in particular, has clarified the standing of Pr¹³⁷.

Each <u>mass separated</u> isotope has been examined to determine its half-life. The results are:

Pr¹³⁹; 4.5 hrs, already well established

 Pr^{135} ; 2.1 \pm 0.05 hrs, a slight increase over earlier values

 Pr^{137} ; 1.5 hrs, confirming earlier McGill value Pr^{136} ; 1.0 \pm 0.15 hrs.

In initial exemination of gamma rays from these <u>mass separated</u> isotopes has forced a revision of some earlier work. Priefly, the results are:

Fr¹³⁹; possible weak 1150 kev; no others > 5% of annihilation radiation

 Pr^{138} ; 160 (new), 300, 800, 1040 kev confirming Dahlstrom, several less intense rays

Pr¹³⁷; none (with intensity > 10% of annihilation radiation)
Pr¹³⁶; none (with intensity > 10% of annihilation radiation)

Owing to the somewhat similar half-lives, the mass separated samples have proved particular advantageous in the study of gamma radiations. Thus previously assigned Pr¹³⁹ rays are cancelled. The 300 kev ray of Pr¹³⁸ has been assigned to other isotopes. Through examination of mass separated Pr¹³⁸ as well as a 2.1 hr conversion electron decay rate it is clear that the 300 kev ray belongs exclusively to Pr¹³⁸. Although the 160 kev gamma has been attributed to Pr¹³⁶ by Handley et al (1954), evidence exactly parallel to the above proves that it belongs to Pr¹³⁸.

The 300 kev. transition is the only one that is strongly converted. Assuming the contribution of all shells beyond the L shell to be approximately 1/4 the L shell contribution, the observed ratio $\frac{K}{L+M+...}=2.2$ gives a value $\frac{K}{L}=2.2$.

Interpolation of the tabulated calculations of Rose and Goertzel (1955) for the internal conversion coefficients, in the case of Z=58

(cerium) and $k = 0.558 \text{ (mc}^2)$, show $\frac{K}{L} = 3.1 \text{ for an E3 transition.}$ The only other multipolarity that gives a value close to the experimental result is an M, which should produce a long half-life for this energy. Thus E3 radiation is favoured.

The K conversion coefficient, from the internal conversion calculations, for a 300 kev E3 transition is $\alpha_{\rm K}=0.125$. Thus even for the extreme case in which 100% of the disintegrations pass through the 300 kev level, the value of the measured K X-ray intensity for Pr¹³⁸ would be only about 10% higher than the true K-capture intensity. Since the limit of error in the calculated branching ratio is about 25%, this contribution is negligible.

Numerical values have been tabulated for log f as a function of the nuclear energy difference " I_0 ", with the atomic mass number Z as a parameter. (Feenberg and Trigg 1950). These values apply for allowed transitions. However, for $\Delta J = 0$, ± 1 transitions, i.e. for all "allowed shape" transitions, the 'f' value is approximately the same (Brysk and Rose 1955).

For first forbidden ($\Delta J = \pm 2$) transitions, there is an energy dependent correction factor. The 'f' value is reduced by a factor of $\frac{\omega_0 - 1}{2(\omega_0 + 1)}$ from the allowed value for the same energy release. For higher orders of forbiddenness, the reduction in the branching ratio is still greater.

The positron maximum energies obtained by Dahlstrom (1953) and by Handley et al (1954) are listed in column 1 of Table II. The nuclear energy differences

$$W_0 = \frac{E(\text{mev}) + 0.511 \text{ (mc}^2)}{0.511}$$

calculated from their values for E, the maximum energies, are listed in Column 2. Column 3 gives the values of W_0 taken from the log f versus W_0 curves, for Z = 59. These curves assume that the transition is allowed.

Thus the results point to agreement with the former workers, and to "allowed shape" transitions, although the possible errors involved do not definitely exclude first forbidden transitions.

However, the branching ratio gives the positron partial half-life 't+' in terms of the total half-life 't'. It is easily shown that

$$t_{+} = (1 + f) t$$

Column 4 lists the logarithms of the values for 't+' calculated from the 'f' and 't' values observed in this work.

Feenberg and Trigg (1950) have also tabulated values for $\log f(N_0, Z)$, the theoretical factor for positron emission, as a function of N_0 , with Z as a parameter. (It should be noted that this 'f' factor refers to positron decay only. It is distinct from the K-capture to positron ratio factor 'f'.)

When multiplied by the positron partial half-life, the positron 'f' factor gives the comparative half-life factor 'f t_+ '.

Values for log f were interpolated for the values of \mathbb{N}_0 obtained in Column 3, which are supported by the independent values in Column 2. The sum of 'log f' + 'log t₊' is listed in Column 5.

These calculations fit well with the values of $\log f t_+$ for allowed transitions, which range from 4.0 to 5.7 for even mass nuclei, and from 4.5 to 6.0 for odd mass nuclei,

From the results of both the f t_+ values and the maximum positron energy values, it appears that the transitions are allowed.

TABLE II

Vass	E (observed Mev)	W _o (calc. from E)	No (calc. from f)	log t ₊	log (ft) ₊
139	1.0 ± 0.1 ½ 1	3.0 ± 0.2	3.2 ± 0.1	5.3 ± 0.1	5.6 <u>+</u> 0.2
138	1.4 ± 0.1 ¹ 1.5 ± 0.1 ₁₁₁	3.8 ± 0.3	3.8 ± 0.2	4.6 ± 0.1	5.4 ± 0.2
137	1.8 ± 0.1 xx	4.5 ± 0.2	4.4 ± 0.3	4.2 ± 0.2	5.3 ± 0.3
136	2.0 ± 0.1 k	4.9 ± 0.2	4.8 ± 0.3	4.0 ± 0.2	5.5 ± 0.3
x - H	Handley et al (1955)				

A newly observed ground state of Ce^{137} of half-life about 9 hrs was indicated in the decay of the 1.5 hr state in Pr^{137} . No evidence for 36 hr Ce^{137} was found via Pr^{137} .

V. Study of Cerium Formed from Praseodymium Decay

(a) Gamma-ray Spectrum

mit - Dahlstrom (1953).

Cerium was bombarded at 40 Mev and the praseodymium activity produced was immediately separated chemically. After a period of 6 hours, during which most of the 1.5 hr. activity in Pr^{137} decayed, the daughter cerium was extracted from the praseodymium parent. Fortunately, only Ce^{137} and 140 d Ce^{139} are produced in appreciable quantities. The latter exhibits only one γ -ray, the 166 kev transition. Thus the γ - and β -ray spectra of Ce^{137} can be studied in detail with a minimum of contaminating radiations.

The cerium daughter, after repeated chemical purification cycles to remove all traces of praseodymium, revealed a γ -ray transition at 440 kev and a very strong X-ray peak. In the cerium so produced, no γ -ray was observed in the 250 kev energy region. If present, it was

less than 1% of the 440 kev peak intensity. No additional γ -rays were found in Ce¹³⁷, and an upper limit of 0.25% of the 440 kev peak intensity was set for higher energy transitions.

The half-life of the 440 kev transition was measured on two occasions as 9.0 ± 0.3 hr. (Fig. 18). The X-ray also decayed with a 9.0 hr period, until it reached about 1% of its original value. Then a weak tail of predominantly 140 d Ce¹³⁹ X-rays became prominent. Since this background correction was so small, the X-ray intensity was measured quite accurately.

The direct mass separations had shown that this 9 hr period was characteristic of the decay in mass 137, and the chemical yield has shown in addition that this activity must be associated with the decay of Ce¹³⁷. No evidence was found for a further daughter activity, which supports the assignment of this 9 hr period to the decay of Ce¹³⁷ to long lived La¹³⁷.

In a portion of the original cerium target, however, a 255 kev peak of low intensity was observed. It was found to have approximately a 30 hr half-life, which supported its association with the 250 kev γ -ray observed by previous workers in Ce¹³⁷; but shown in this thesis to be an isomeric state.

(b) The Conversion Electron Spectrum

A chemically extracted cerium daughter source, produced from a 50 Mev bombardment, was studied in the thin lens spectrometer.

The Auger electrons provided the only significant peak. However, a careful manual scan was made over the momentum region corresponding to about 440 kev unconverted γ -ray energy. A very small intensity was observed at the appropriate position.

(c) Calculations and Discussion

The new 9 hr state in Ce¹³⁷ appears to decay by electron capture, as is indicated by the large X-ray intensity. It presumably goes to the ground state of long lived Ia¹³⁷. There is a small branching to a 440 kev level in La¹³⁷.

The absolute disintegration rate for the 440 kev γ -ray is easily obtained from the observed peak intensity and the efficiency of counting.

However the absolute intensity for electron capture is more difficult to find. The branching ratio to the 440 kev level can be determined from these two quantities. Since the branching is only a small part of the capture events, and since the 440 kev transition conversion was found to be very small, K-conversion X-rays will be insignificant. Thus the measured K X-ray intensity ${}^{1}N_{K}{}^{1}$, corrected for the counter efficiency ${}^{1}S_{K}{}^{1}$ and the fluorescent yield ${}^{1}C_{K}{}^{1}$ gives the primary number of K shell vacancies ${}^{1}V_{K}{}^{1}$, due to K-capture. Then if the K- to total capture ratio is known, the number of capture events can be calculated.

The theoretical transition probabilities for electron capture from the K and L shells have been studied by Brysk and Rose (1955), applying corrections for the finite size of the nucleus and for screening.

The disintegration energy for electron capture is difficult to determine, but fortunately the K-capture fraction of the total capture varies slowly with the disintegration energy, for all values considerably above the K-capture threshold. Furthermore the L_I subshell contribution, which is responsible for most of the L shell contribution, is a nearly constant fraction of the K-capture, again for energies considerably above the K-capture threshold.

The K- to total=capture ratio used in these calculations on Ce¹³⁷ was obtained from the above data by assuming a zero energy difference between Ce¹³⁷ and La¹³⁷. The theoretical data is for an "allowed" transition.

Since a branching to a 440 kev state ($k = \frac{440}{511} = 0.85$) takes place, the nuclear energy difference 'W' cannot be less than W' = $\frac{440-511}{511} = -0.15$. Furthermore, since there is no positron emission, the energy difference cannot be much above 1.0.

Fortunately, the $\frac{L_1}{K}$ ratio varies very slowly in this region and as a result the assumed value is not critical. For $W_0=0$, the ratio $\frac{L_1}{K}=0.13$, and $\frac{L_{11}}{K}=0.01$. The L_{111} contribution is negligible except for a first forbidden unique transition, where it is about 12% of the L_1 value.

For the higher shells, an estimate of about 7% of the K shell contribution was made, assuming a simple variation as the inverse cube of the principal quantum number 'n' for the transition probability. In this manner a K- to total-capture ratio of

$$\frac{K}{E.C.} = \frac{1}{1.21}$$

was estimated. The accuracy of this ratio should be sufficient for the calculations to be made.

The absolute intensity of 440 kev γ -rays 'I' equals the number of capture events to the excited state. The total number of capture events equals 1.21 times the total number of K-capture events. Thus the branching to the 440 kev level is, (using Eqn 2, p. 48)

f =
$$\frac{I_{\gamma}}{1.21} \frac{X_{K}}{\omega_{K}} = \frac{\frac{N_{\gamma}}{\delta_{\gamma}}}{1.21 \frac{N_{K}}{\omega_{K}} \delta_{K}}$$
 (3)

The observed peak counting rates at 3 cms were N = 140 cps and N $_{\rm K}$ = 15400 cps.

A complication due to the detector itself arises in estimating the efficiency for K X-rays. An accurate value of ${}^1\delta_K{}^1$ is hard to determine, as explained below.

For energies below 100 kev, the efficiencies given for the detector used (Skarsgard 1955) are the computed total counting efficiencies of McGowan (1954). These computed efficiencies are approximately equal to the photoelectric efficiencies at low energies. However, the photoelectric effect gives rise to both the main peak and to the peak which occurs at 28 kev lower energy, due to the escape of iodine X-rays from the NaI(T1) crystal. For cerium or lanthanum X-rays, which are about 33 kev in energy, this "escape peak" cannot be observed, since its energy is too low to be detected above the amplifier noise. This unknown part of the total intensity is not detected.

An experiment was performed in which a source of cerium X-rays was pressed tightly between two identical 1.5 in. × 1 in. NaI(T1) detector units placed end to end. The combined outputs were 15% greater than the sum of the two counter rates when apart. This indicated that 15% of the total main peak intensity was escaping into the opposite crystal. This, however, does not represent the entire escape peak, since some losses will occur due to incomplete geometry, and to absorption in the aluminum covers.

A similar experiment was performed with tantalum X-rays, which are approximately 57 kev in energy. Here, both the 57-28 escape peak and the peak due to 28 kev iodine X-rays from the opposite detector were observed. This showed that 60% of the escaped X-rays were detected in the opposite counter.

With a single counter, the escape peak for tantalum X-rays was 22% of the main peak at 0 cms, and 16.5% at 3 cms.

Assuming that the efficiencies are about the same in both cases, this would indicate that

$$\frac{15}{100} \times \frac{100}{60} \times \frac{16.5}{22} = \frac{19}{100}$$

or 19% of the cerium X-rays. were not present in the photoelectric peak at 3 cms. This means that the ${}^{1}\delta_{K}{}^{1}$ should be reduced by 19% from the total counting efficiencies.

A further complication arises from the fact that while cerium X-ray components are all above the iodine K-edge, lanthanum components are not. The La Ka $_2$ (i.e. K-L $_{11}$) component is below the iodine K-edge in energy, and thus it contributes nothing to the escape peak.

The ratios of the intensities of the K α_1 : K α_2 : K β are respectively about 2:1:1. (Richtmeyer and Kennard). Thus only 3/4 of the lanthanum X-rays contribute to the escape peak and as a result the efficiencies for lanthanum X-rays should be approximately $(3/4 \times 19 = 15\%)$ too high.

Correcting for this factor and applying ω_{K} = 0.87 for lanthanum X-rays (Bergstrom 1955), gives the branching to the 440 kev level

$$f = 0.031$$

On another occasion a value of f = 0.029 was obtained.

Thus about 3% of the total capture events are to the excited 440 kev level.

(d) Conclusions

A previously unknown 9 hr state has been definitely assigned to cerium by chemical yields, and to mass 137 by isotope separation.

A part of the work on Ce¹³⁷ described herein has been done independently by Brosi and Ketelle (1955). The connection with Pr¹³⁷ is not disclosed by these authors, and their evidence is in other respects somewhat limited.

In a well-separated praseodymium sample of any age there was no evidence for the 250 kev 36 hr γ -ray attributed to Ce¹³⁷, and for which a formidable array of evidence exists.

However, in the original target a weak 255 kev γ -ray with about the required period indicated that if this γ -ray was associated with Ce¹³⁷, it must have been produced by (p,pxn) reactions rather than as a result of the decay of Pr¹³⁷.

VI. Study of Cerium 137 Produced by Proton Reactions on Lanthanum

(a) The γ-ray Spectrum.

The γ -ray spectrum of the cerium activity extracted from lanthanum bombarded with 30 MeV protons was studied on several occasions. At this bombardment energy, which is well below the threshold for Ce^{135} , the only other cerium activity produced besides the $La^{139}(p,3n)Ce^{137}$ reaction, is a relatively small amount of Ce^{139} . This facilitates the study of the γ -radiation associated with Ce^{137} .

The γ -ray spectrum revealed very intense X-rays. Strong 255 and 440 kev γ -rays were observed, as well as a weaker intensity peak at about 810 kev.

The half-life for the 255 kev γ -ray was measured over 5 half-lives, giving a 34.4 \pm 0.3 hr period. The 800 kev transition displayed the same half-life. The X-rays and 440 kev γ -ray peaks showed a composite decay. After an initial short life which was fitted to 9 hrs, they also decay with a 34.4 hr period. No activity which could be attributed to the decay of La¹³⁷ was found.

No positrons were observed. The upper limit on unobserved high energy γ -rays can be set at 0.5% of the 800 kev transition. An unsuccessful search was also made for low energy γ -rays down to the limits of detection (about 10 kev).

The ratios of the various absolute intensities were calculated after equilibrium was reached with the 34.4 hr half-life. The ratio averaged over several runs of the X-ray: 255 γ : 440 γ : 810 γ was 1.00: 0.081: 0.020: 0.0045. The accuracy of the intensities for the X-rays, 255 and 440 γ -rays, should be equal to the accuracy of the efficiency values, or about 10%. For the weaker 810 kev transition, the accuracy should be better than 20%. The total photoelectric efficiency for the X-rays has been corrected for the escape peak factor discussed in an earlier section.

An attempt was made to observe activity due to the ${\rm La}^{137}$ daughter of ${\rm Ce}^{137}$.

A 4 hour bombardment of La produced very intense Ce^{137} activity. The decay of a small aliquot of the separated cerium was followed. After 5.5 days, when the Ce^{137} fraction had decayed to about 5% of its initial value, the La^{137} daughter formed was separated out chemically and subjected to repeated purification cycles to eliminate all the cerium activity. Apart from a very weak 490 kev γ -ray, which decayed with a relatively short half life of about one week, no activity was observed.

The activity due to Ce^{137} immediately present after bombardment was calculated to be about 7×10^7 counts per sec. Thus a weak transition with a one week half-life must be interpreted as due to some extraneous activity.

No X-rays or positrons were observed, indicating that the decay of ${\rm La}^{137}$ to stable ${\rm Ba}^{137}$ is extremely long lived.

Assuming losses of 25% in the chemical extractions, and a lower limit of 0.1 cps for the detection of 33 kev X-rays or annihilation radiation, both of which are conservative estimates, gives the lower limit for the

half-life of La 137 to be about

$$\frac{5 \times 10^7}{0.1} \times \frac{34.4}{8250} \ge 1 \times 10^6 \text{ yrs.}$$

(b) The Conversion Electron Spectrum

(1) The thin-lens spectrometer results.

Sources of Ce^{137} produced by 30 Mev bombardments on lanthanum were scanned in the thin lens spectrometer. Extremely strong conversion electron peaks due to the 255 kev transition were observed. The half-lives were 34.4 \pm 0.3 hrs. Fig. 19 illustrates the decay of the K-conversion peak. The K/L+M+... ratio was measured as 2.3 \pm 0.1. Fig. 20 shows a typical conversion spectrum for the 255 kev transition.

The comparatively weak conversion electron peaks for the 440 \pm 5 keV γ -ray are illustrated in Fig. 21. The K/L+M+... ratio was 5.0 \pm 0.5.

The very weak conversion peaks due to the 800 kev transition were counted manually over several days, from a very strong source, and the results were then corrected to one standard time. Fig. 22 shows the conversion spectrum. This conversion spectrum revealed that there were actually a group of several closely spaced weak transitions present. The strongest component is due to a 812 ± 7 kev transition. As illustrated in the figure, the overlapping of lines makes the assignment of K/L ratios difficult. However, for the strongest component, the K/L+M+... ratio appeared to be 6.3 ± 1.2 .

The intensity of the group at about 800 kev is very low. The ratios of the K-conversion intensities of the 255, 440, and 812 kev respectively averaged 1:5.35 \times 10⁻⁴:2 \times 10⁻⁵. These ratios should be accurate to within 10%.

A manual scan showed no low energy conversion peaks above 10 keV (other than those due to the Auger electrons) which were detectable above the 200 cpm background. This was for a source giving 2×10^6 cpm in the 255 γ -ray K-conversion peak, and thus the limits on low energy conversions can be made very small.

A possible transition from some of the 812 kev group to the 440 level were searched for. No conversion electrons of the appropriate energy were found, and the upper limit for such a transition can be set at less than 1% of the 440 kev K-conversion intensity.

By comparing the intensities of K-conversion peaks to the absolute γ -ray intensities, the K-conversion coefficient can be derived, if the transmission efficiency of the thin-lens spectrometer is known. This efficiency for the instrument used is about 1% for a normal sized source.

Applying a 1% transmission efficiency to the intensity of the K-conversion of the 255 kev γ-ray gave for the conversion coefficient

$$\alpha_{K} = \frac{N_{K}}{N_{\gamma}} = \frac{1.51 \times 10^{6} \text{ cpm}}{3.18 \times 107 \text{ cpm}} \times 100 = 4.8.$$

This value is accurate to within 30%.

Comparison with the K-conversion coefficients for Z = 58 and k = 0.5 for various multipolarities indicates that only an M4 transition is consistent with this result. (Rose and Goertzel 1955).

(2) The 180° Spectrograph Conversion Results

It has been found that the decay of Pr^{137} gives rise only to the 9 hr decay in Ce^{137} , while Ce^{137} produced directly by proton bombardment of lanthanum exhibits a 34.4 hr period in addition. The 440 kev γ -ray is present in both cases, whereas the 255 kev γ -ray is characteristic of the simple 34.4 hr decay.

These facts throw some doubt on the validity of the previous assignment of the 255 kev γ -ray to an excited state in La¹³⁷, following electron capture in Ce¹³⁷, and suggest its assignment to a long lived isomeric state in Ce¹³⁷.

The most direct method of identifying in which element the 255 kev transition exists is to make accurate measurements of the conversion electron energy differences and compare these with the corresponding electron binding energy differences in the two elements.

These measurements were obtained with a high resolution (0.2%) semicircular spectrograph. The source was prepared by the novel teflon trough method described earlier.

The instrument was calibrated with the standard F, I, L, lines in the thorium $(B + C + C^{11})$ spectrum. The energies of the conversion lines were then calculated from the measured radii of curvature and the calibrated magnetic field.

The K, L_1 , L_{11} , L_{111} , M and N shell conversion lines of the 255 keV γ -ray were obtained. The energies obtained for these lines are given in Table III.

TABLE III

<u>Line</u> K L₁ L₁₁ L₁₁₁ M N

<u>Energy</u> (kev) 214.02 248.13 248.46 248.92 253.33 254.41

These energies are accurate to about \pm 0.2 kev.

In Table IV the energy differences are compared with the electron binding energy differences in cerium and lanthanum.

TABLE IV

Shells involved	Measured differences (kev)	Electron energy Ce (kev)	differences La (kev)
K - L ₁	34.11	33.87	32.66
K - L ₁₁	34.44	34.26	33.02
K-L ₁₁₁	34.90	34.70	33.43
K - M	39.31	39.2	37.8
K-N	40.39	40.2	38.7
L ₁₁ -L ₁	0.33	0.39	0.36
L ₁₁₁ -L ₁	0.79	0.83	0.77
L ₁₁₁ -L ₁₁	0.46	0.44	0.41

On the basis of the comparison, especially of the K-M and K-N differences which are close to the total K binding energies in value, the 254.5 keV γ -ray is converted in Ce¹³⁷.

For the 254.5 kev conversion electron plate obtained, estimates were made of the intensity ratios for the L lines by visual examination of the plate itself, and by measurements on the peak heights obtained on a microphotometer trace. (Fig. 23).

Table V lists the estimated L conversion coefficient ratios, the K/L ratio measured in the thin-lens spectrometer, and for comparison, the values of these ratios for M3, M4, and M5 transitions for Z = 58 from the theoretical values of Rose et al (1955).

TABLE V

Ratio	Measured and estimated	Calculated M3	Calculated M4	Calculated M5
K/L	2.9 [*]	4.4	3.0	1.8
$\frac{L_1}{L_{11}}$	3 to 6	5•7	4.3	3.5
$\frac{L_1}{L_{111}}$	1.5	4.1	1.75	1.0
L ₁₁	0.25 to 0.5	0.7	0.41	0.3

The K/L = 2.3 value obtained from the thin-lens spectrometer results, corrected for a 25% M+... contribution to the L intensity.

The low order multipoles of either character are eliminated on the basis of the long half-life involved. The higher electric multipoles are eliminated by the relative smallness of the L_{11} contribution. A comparison of the measured with the calculated ratios, particularly the K/L ratio which can be measured quite accurately, indicates that the 255 kev γ -ray is a M4 transition.

This result is consistent with the result obtained earlier for the calculation of the K-conversion coefficient.

VII. Investigation of Coincidences

A study was made of the coincidence relationship of the 440 and 255 kev γ -rays to the X-rays. The block diagram in Fig. 24 illustrates the "fast-slow" coincidence circuit employed.

The lead baffle prevents the occurrence of false coincidences due to radiation scattered from one detector to the other. The detectors, which are approximately identical, are placed equidistant from the source. The output of detector 1 is amplified and fed into the final gating circuit. The output of detector 2 is fed through a single channel pulse height analyser to a slow coincidence circuit.

The pulses from both detectors are sampled in the fast coincidence circuit which, by the use of a delay line and diode detector, presents a very short resolving time. When pulses from the two detectors are coincident within the limits of this short resolving time, a triggering pulse is fed to the slow coincidence unit. This permits the pulse from detector 2 to pass through the slow coincidence unit, provided it is of the proper energy to go through the single channel window. Coincident

pulses entering the gating circuit from the slow coincidence output and from detector 1 are let through and are recorded as events. The resolving time was set at 50×10^{-9} sec.

By introducing a large delay into the output of the fast coincidence unit, true coincidences can be prevented, and the chance rate 'Nch' can thus be obtained.

The events were counted on a scalar, and also were fed into the kicksorter to obtain the energy distribution.

(a) The 440 kev γ-ray

The single channel window was set on the 440 kev γ -ray peak (Fig. 25). The singles counting rate 'N2' of all pulses from detector 1 was 2.68×10^5 cpm at a standard time used in the calculations. The channel singles counting rate 'N1' of all pulses passing through the window was 2400 cpm. The measured coincidence rate (true plus chance) was $\frac{206}{60} = 3.4$ cpm. By introducing 0.4×10^{-6} sec delay to the fast coincidence output, true coincidences are eliminated and only the chance rate is obtained. This gave $\frac{36}{60} = 0.6$ cpm. This is consistent with the calculated rate,

 $N_{ch} = 7 N_1 N_2 = 50 \times 10^{-9} \times 2.68 \times 10^5 \times \frac{2400}{60} = 0.55$ cpm. The result indicated that 2.8 cpm true coincidences occurred.

Consider the case of coincidences between the 440 kev γ -ray and X-rays. The coincidence rate is

$$N_c = N \delta_2 \delta_1$$

where N is the absolute intensity of the 440 kev y-ray

 δ_2 is the efficiency of detector 2 for the $\gamma\text{-ray}$

 $\boldsymbol{\delta}_1$ is the efficiency of detector 1 for X-rays.

Now N δ_2 = N $_{\gamma}$, the γ -ray photoelectric peak intensity in detector 2, which will be approximately the same as that in detector 1. The photoelectric peak intensities measured in detector 1 for the 440, 255, and the X-ray respectively, were 951, 9080, and 152,000 cpm, when corrected to the standard time taken for these measurements.

For a distance of about 13 cms from the detectors to the source, the X-ray efficiency of detector 1 was estimated to be about 0.004.

This gives $N_c = 951 \times .004 = 4.0$ cpm compared with the observed rate of 2.8 cpm. Considering the inaccuracies involved, and the fact that the fast circuit discriminates somewhat against the low amplitude X-ray pulses, this result indicates that the 440 keV γ -rays are coincident with the X-rays.

(b) The 255 Kev γ-ray

The "window" was set for the 255 kev peak (Fig. 25). Care was taken to exclude the 166 kev Ce 139 γ -ray from the window region.

The true plus chance rate obtained from a 10.8 hr count gave 10.32 cpm. With the delay inserted, the chance rate was measured for 42 minutes, giving 5.12 cpm. This indicated that 5.2 cpm from true coincidences were occurring.

The singles counting rate through the window was 12,010 cpm. If the 255 transition were in coincidence with X-rays, the coincidence rate would be N_c = 12010 × 0.005 = 60 cpm. This showed that, except for a small component, there were no coincidences with the 255 keV γ -ray.

In partial explanation of the above apparent coincidences, the Compton continuum of the 440 kev γ -ray in the energy range of the window will be in coincidence with the X-rays. Estimating this portion of the continuum as about 75% of the photoelectric peak intensity accounts for at least 1/2 of the observed rate.

Fig. 26 shows the energy distribution of the coincidences taken for the 10.8 hr count. The first two channels, containing the X-ray peak, plus some noise in channel 1, have been reduced in scale by a factor of ten. The distribution of the increase over chance under the whole window illustrates the effect of the Compton continuum, since the 255 kev γ -rays cannot be in coincidence with themselves.

(c) Conclusions

The results of the 440 kev γ -ray coincidence experiment, as well as the effect of its continuum in the 255 kev window, both show that the 440 kev transition is coincident with X-rays, as is to be expected.

The 255 kev γ -ray resulting from the isomeric transition in Ce¹³⁷ did not produce coincidences with X-rays, which again is to be expected. A small effect was observed at least half of which is explained by the Compton continuum.

VIII. A Proposed Decay Scheme for the Mass 137 Chain

It has been shown that 1.5 hr Pr^{137} decays by an allowed transition to a 9.0 hr ground state in Ce^{137} . This state then predominantly decays to the ground state of La^{137} , with a small branching to a 440 kev excited state. No other γ -rays were found associated with this mechanism.

Since the ratio of the 255 kev to 440 kev K-conversion peak is exceptionally high in the cerium from a lanthanum target, this ratio may serve as a very sensitive detector of any branching from Pr¹³⁷ to Ce^{137m}. When this test was made on the cerium produced from decay of Pr¹³⁷, the ratio fell to the trace value of 0.8% - a value which indeed may represent only chemical impurity due to Ce^{137m} produced by (p,pxn) reactions. Thus the value 0.8% represents only an upper limit for branching to Ce^{137m}.

The various experiments conducted on 5gCe₇₉ produced from lanthanum bombardments all support the isomeric transition assignment. This result is consistent with predictions based on the tehaviour of other isotopes with odd values of 'N' which lie just below "magic numbers". These "islands of isomerism" give rise to long lived E3 or M4 isomers, for odd 'A' isotopes. (Goldhaber and Hill 1952).

Assuming the 255 kev transition has an M4 multipolarity, and using the K-conversion coefficient $\alpha_{\rm K}=5.63$ obtained from the values of Rose et al (1955), the K-conversion coefficient for the 440 kev transition may now be obtained quite accurately.

The ratios of the γ -ray and γ -ray peaks for the 440 kev and 255 kev transitions, combined with $\alpha_{\rm K}=5.63$ for the 255 transition, give $\alpha_{\rm K}=0.012\pm0.002$ for the 440 kev transition. The appropriate interpolated theoretical values are $\alpha_{\rm K}=0.010$ for E2, and $\alpha_{\rm K}=0.017$ for M1.

No other multipolarities are close to the experimental values.

The K/L ratio excludes an MI in favour of an E2 transition. The theoretical values are K/L = 6.0 for E2, and K/L = 8.1 for MI. The experimental value, assuming a 25% M4... contribution, gives K/L = 6.25. This excludes a predominantly MI transition, but a small admixture of MI to the E2 transition would be possible.

For the SL2 'tev group, the γ -ray spectrum is not resolved, so that estimates of the K-conversion coefficients of the components cannot be made properly. The K/L ratio of 7.9 \pm 1.5 for the main 812 kev component has such large limits of error that a multipolarity cannot be assigned on this basis.

The branching to the S12 kev group as a whole can be easily calculated from the relative intensities of its γ -ray to that of the 255 kev transition.

The total disintegration rate ${}^{\dagger}I_{1}{}^{\dagger}$ of the Ce^{137m} state is

$$I_1 = (1 + \alpha_T) I_{\gamma}$$

where $\alpha_{\!\scriptscriptstyle T\!\!\!\!/}$ is the total conversion coefficient

I $_{\Upsilon}$ is the 255 kev γ -ray intensity.

(This ignores the negligible 312 kev branching contribution).

You $\alpha_{\rm T} = (1 + \frac{\text{L+...}}{\text{M}}) \cdot \alpha_{\rm M}$, which is calculated from the conversion spectrum results and $\alpha_{\rm M} = 5.63$.

From the measured intensity ratio of the 255 kev and 312 kev γ -rays, the branching is obtained. (The very weak conversion electron contribution of the 312 kev group is again ignored). The value for the 312 kev group branching as a whole is

The branching to the 440 kev level can be obtained in an analogous manner. In this case, however, the disintegration rate I_2 of the ground state, in equilibrium with the 34.4 hr period, is $I_2 = \frac{\lambda_2}{\lambda_2 - \lambda_1}$ I_1 where λ_2 and λ_1 are the appropriate ground state and isomeric state decay constants respectively.

Applying the measured values of the 255 and 440 γ -ray intensities the value of the 440 branching ratio is

$$f = 2.0\% \tag{4}$$

This result assumes, apart from the M4 K-conversion coefficient, only the K/L+... ratio, the half-lives, and the γ -ray intensities.

The 440 branching ratio can be obtained independently in terms of the X-ray intensities, without making any assumption concerning an M4 transition. Again

$$I_1 = I_{\gamma} (1 + \alpha_T) = I_{\gamma} + \frac{\alpha_T}{\alpha_K} I_{k_1} / \omega_K$$

where I_{k_1} is the Ce^{137m}. K X-ray intensity, and ω_K is the fluorescent yield. The total number of capture events to La¹³⁷ is $I_2 = 1.21 \ I_{k_2}/\omega_K$ where I_{k_2} is the La¹³⁷ K X-ray intensity and 1.21 is the total to K-capture ratio.

Ignoring the small δ_K and ω_K differences between cerium and lanthanum, the X-rays can be added indiscriminately. From the ratio of the total K X-ray intensity $I_k = I_{k_1} + I_{k_2}$ to I_γ , the branching ratio can be obtained by solving the equations above, giving

$$f = 3.0\% \tag{5}$$

The values obtained for 'f' by two independent computations involving the X-ray efficiencies are 3.1% for the ground state only, (Eq'n 3) and 3.0% for the case of the ground state in equilibrium with the isomeric transition (Eq'n 5).

This illustrates the internal self consistency of the assumed scheme.

Both the X-ray calculations give a 15 larger branching than the value of 25 obtained in Eqn (4), assuming an M4 transition. The latter value is probably the most accurate, since it involves no approximations concerning the X-ray efficiencies.

The slight discrepancy is probably due to too low an estimate of the X-ray escape peak. In addition, the validity of the generally assumed values for the fluorescent yield have been questioned (Pruett and Milkinson 1954). In any event the discrepancy is a minor one.

A tentative decay scheme is illustrated in Fig. 27.

BIBLIOGRAPHY PART B

- 1. Bergstrom, I. 1955. "Beta and Gamma-Ray Spectroscopy, Kai Siegbahn (Editor), North-Holland Co., p. 630.
- 2. Brosi, A.R. and Ketelle, B.H. 1955. Phys. Rev. 100, p. 169.
- 3. Brysk, H. and Rose, M.E. 1955. ORNL-1830.
- 4. Chubbuck, J.B. and Perlman, I. 1948. Phys. Rev. 74, 982.
- 5. Dahlstrom, C.E. 1953. "Neutron Deficient Isotopes of Praseodymium", Ph.P. Thesis, McGill University, 'ugust 1953.
- 6. Dewire, J.M., Pool, M.L., and Kurbatov, J.D. 1942. Phys. Rev. 61, 564.
- 7. Feenberg, E. and Trigg, G. 1950. Rev. Mod. Phys. 22, 399.
- 8. Goldhaber, M. and Hill, R.D. 1952. Rev. Mod. Phys. 24, p. 179.
- 9. Handley, T.H. and Olson, E.L. 1954. Phys. Rev. 96, 1003.
- 10. Hill, R.D. 1951. Phys. Rev. <u>82</u>, 449.
- 11. Hollander, J.M., Perlman, I., and Seaborg, G.T. 1953. "Table of Isotopes", Rev. Mod. Phys. 25, 469.
- 12. Inghram, M.G., and Hess, D.C. 1948. Phys. Rev. 74, 627.
- 13. Keller, H.B., and Cork, J.M. 1951. Phys. Rev. <u>84</u>, 1079.
- 14. McGowan, F.K. 1954. Phys. Rev. 93, 163.
- 15. Pruett, C.H. and Milkinson, R.G. 1954. Phys. Rev. <u>96</u>, 340.
- 16. Richtmyer and Kennard, "Introduction to Modern Physics", 1947, Fourth Ed., McGraw-Hill.
- 17. Rose and Goertzel (See Siegbahn (1955), and later unpublished data).
- 18. Siegbahn, K. 1955, "Beta-and Gamma-Ray Spectroscopy", (Editor), North-Holland Co.
- 19. Skarsgard, H.M. 1954. N.R.C. Studentship Report Skarsgard, H.M. 1955. Ph.D. Thesis, McGill University
- 20. Stover, B.J. 1951, Phys. Rev. <u>31</u>, 8.

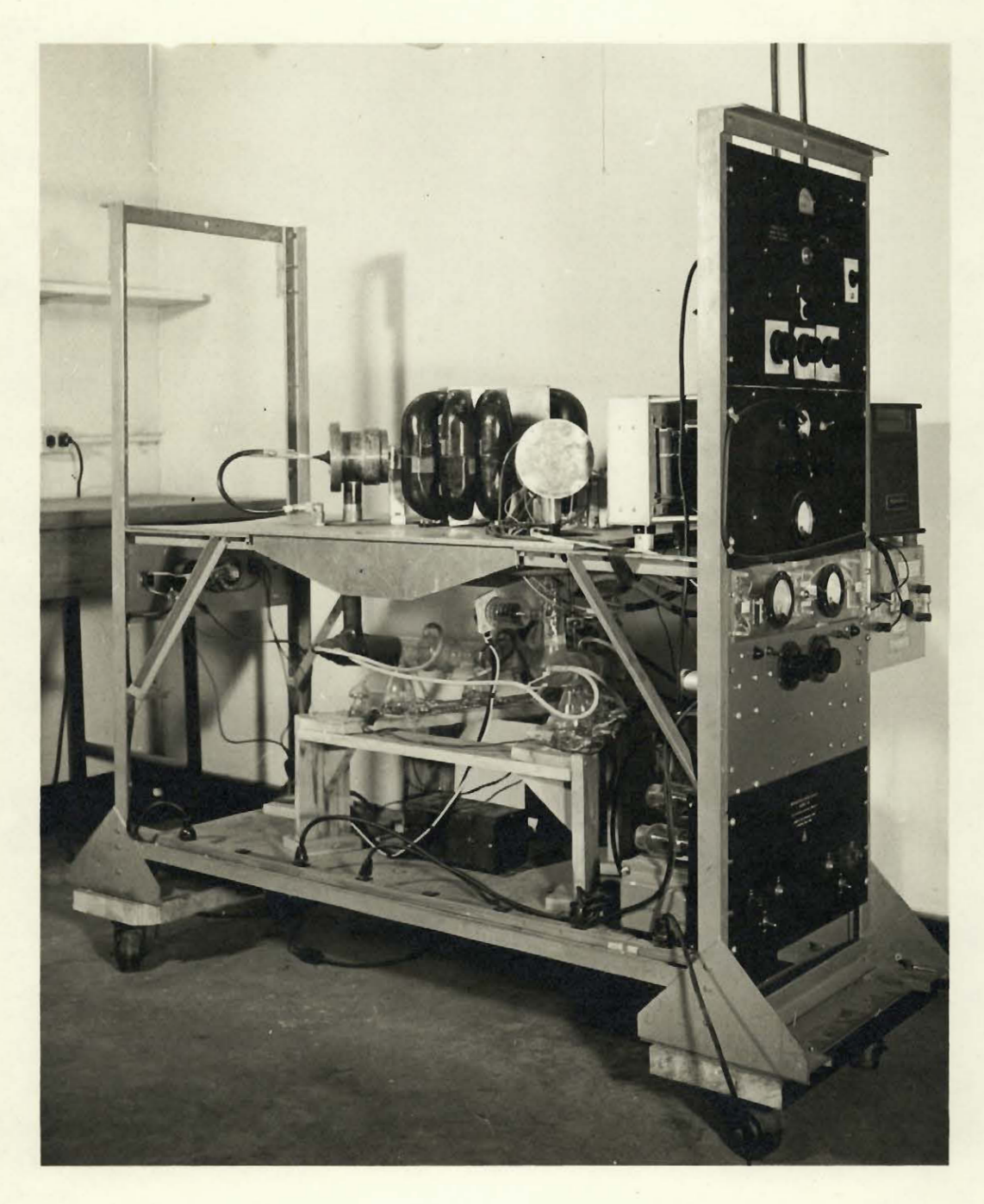
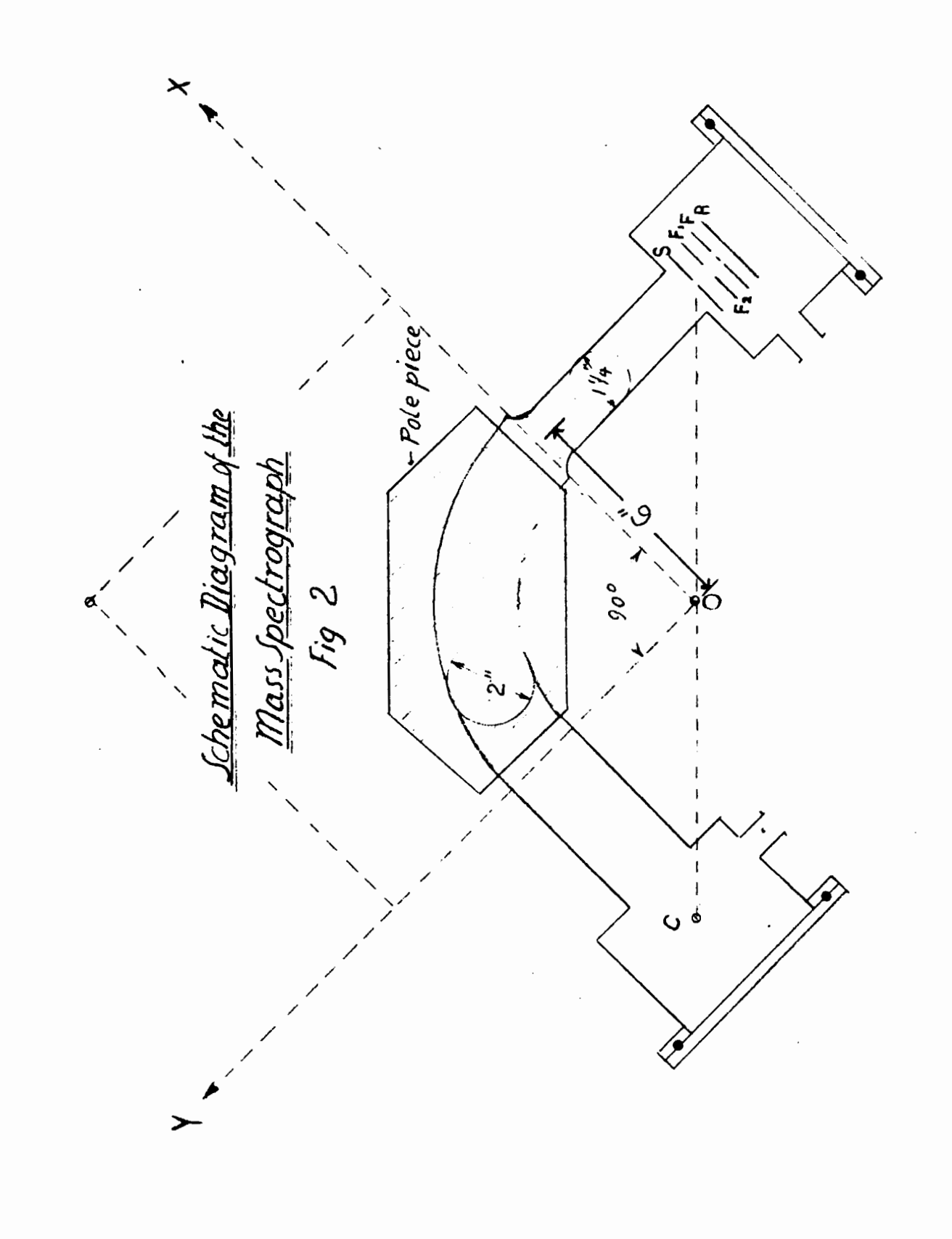
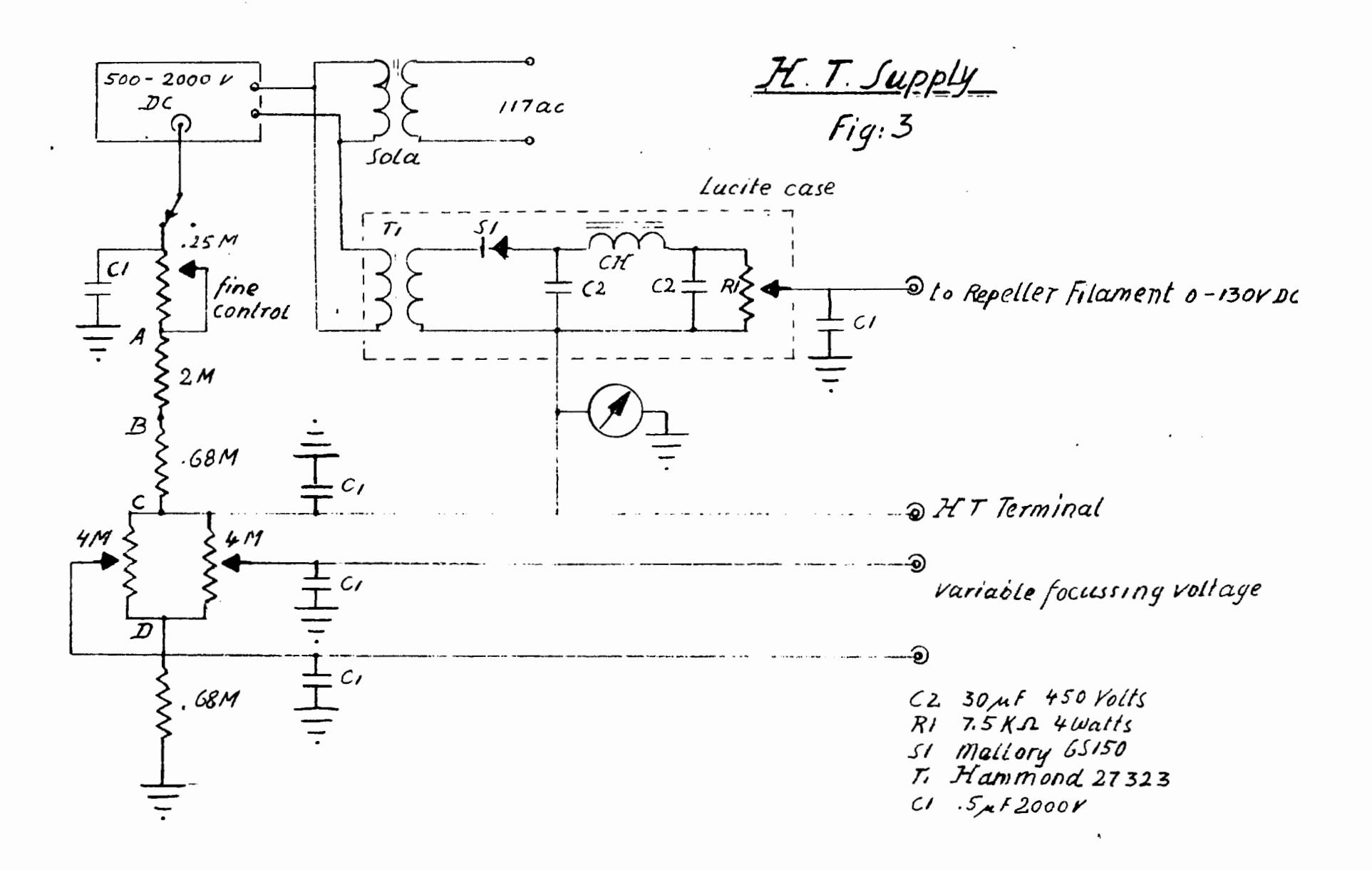


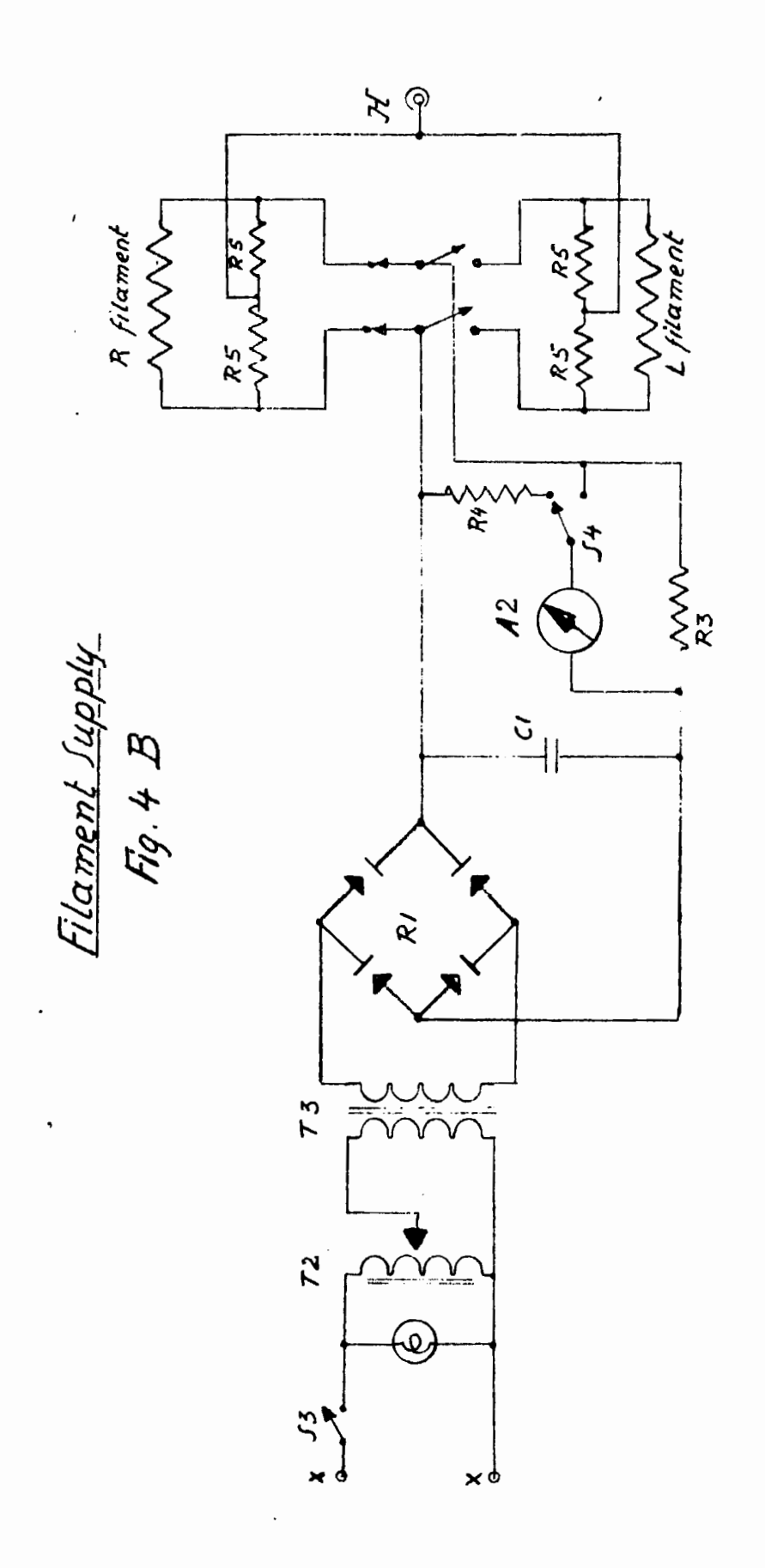
FIGURE 1. The Mass Spectrograph



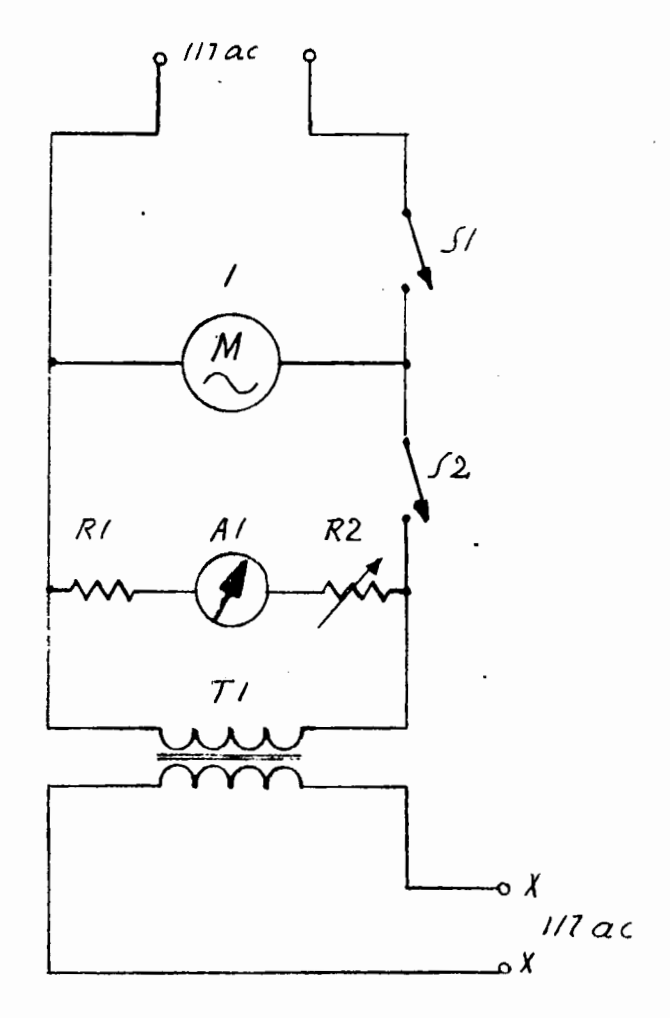


Filament 3 72 23

Filament Supply Fig.4 A



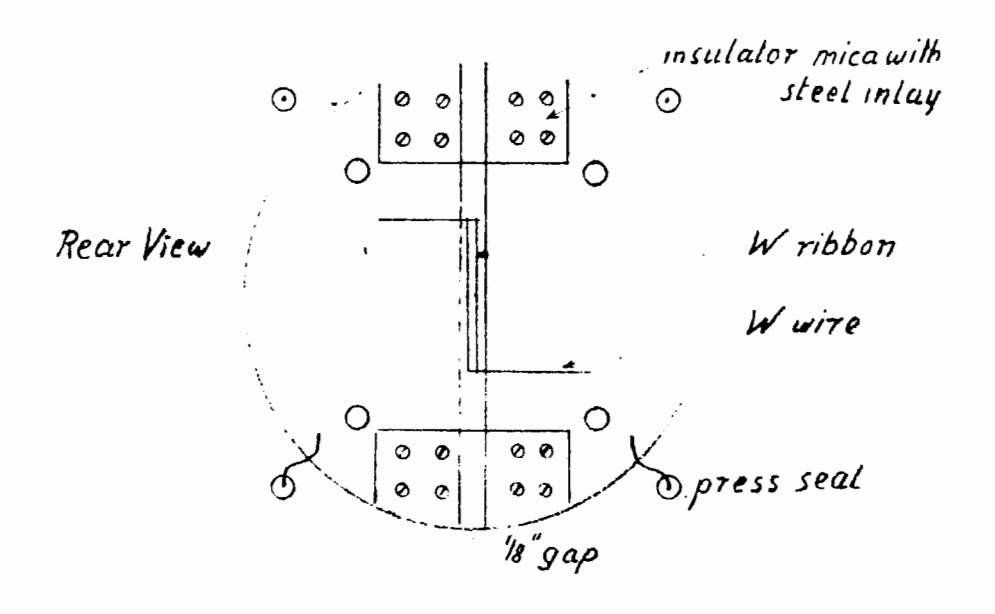
Filament Supply Fig. 4 (



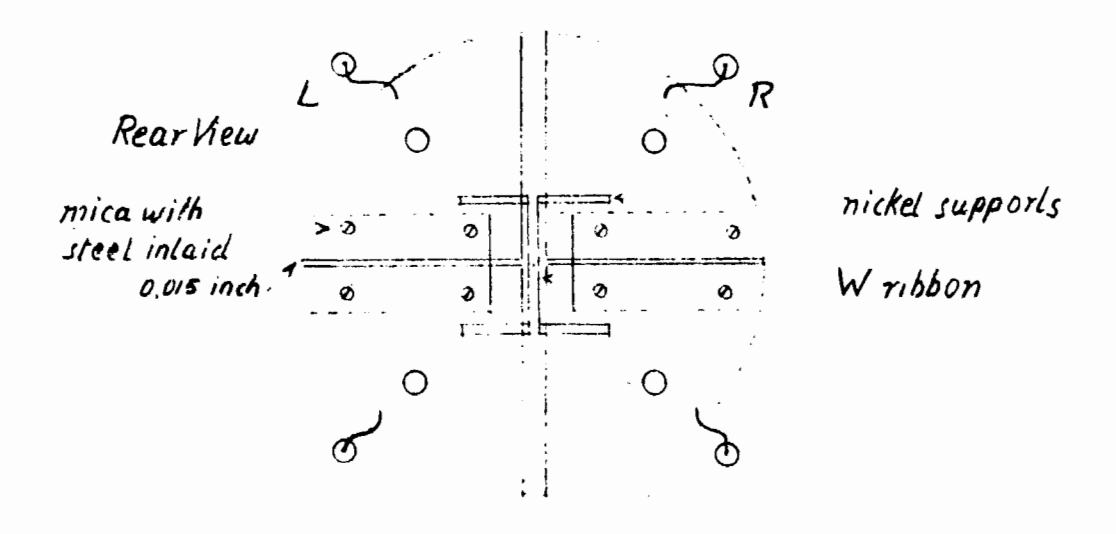
I fore pump
RI diffusion pump heaters
AI diffusion pump heaters
AI diff pump heater current
R2 heater current control
SI forepump switch
S2 diff. pump switch
TI 60VA Sola const.voltagetransformer

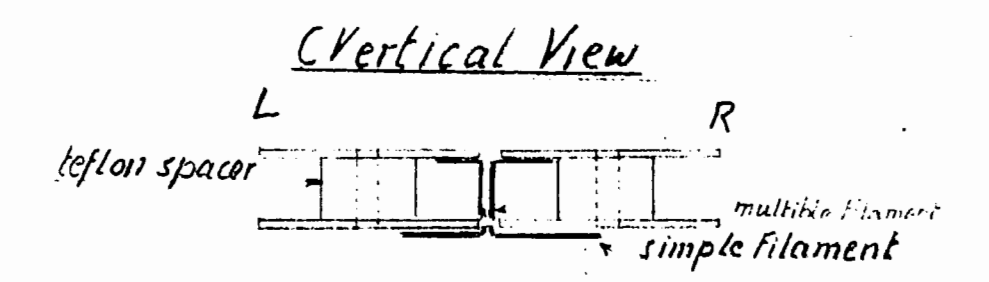
A Simple Filament

Fig. 5



B Multible Filament





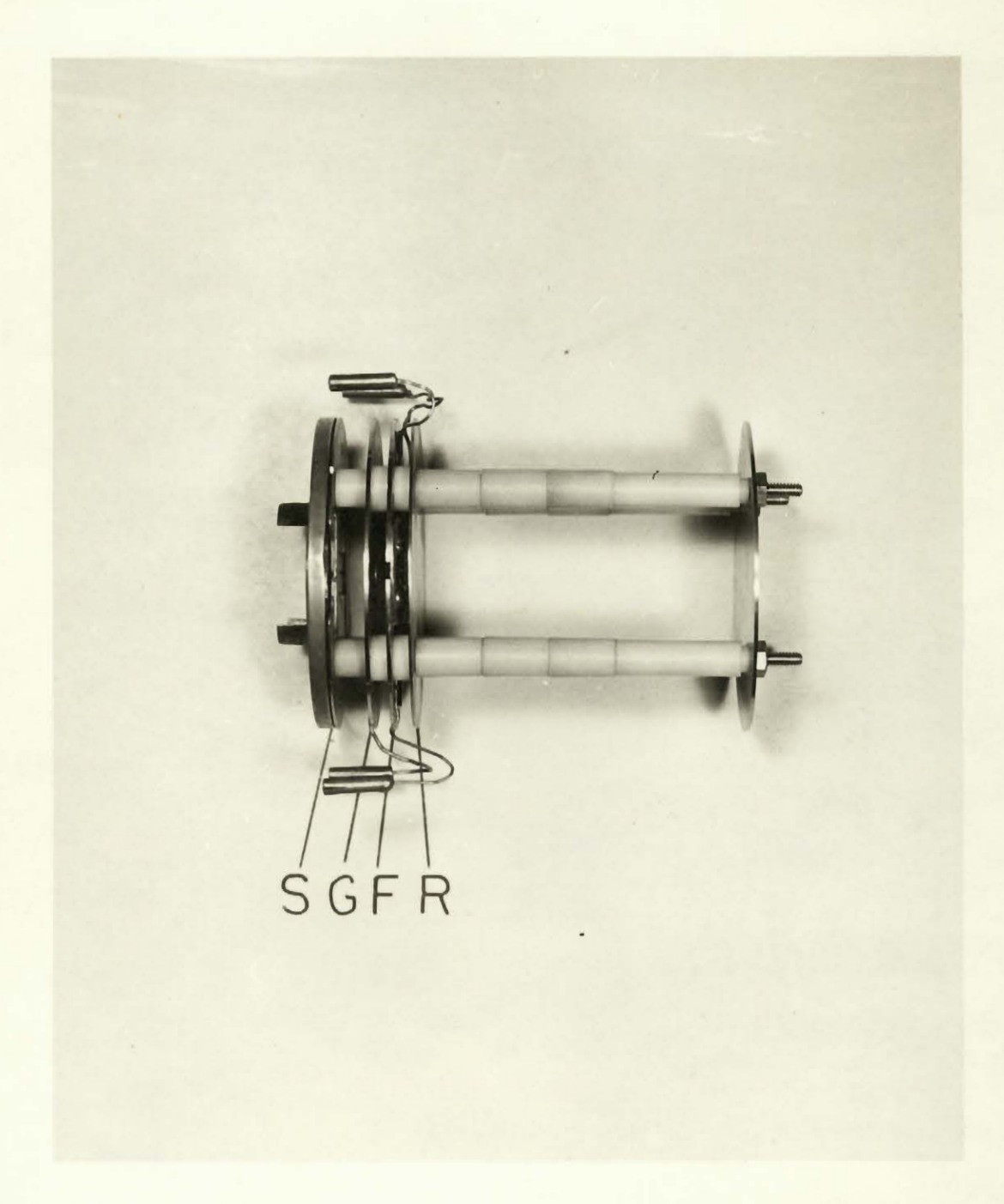
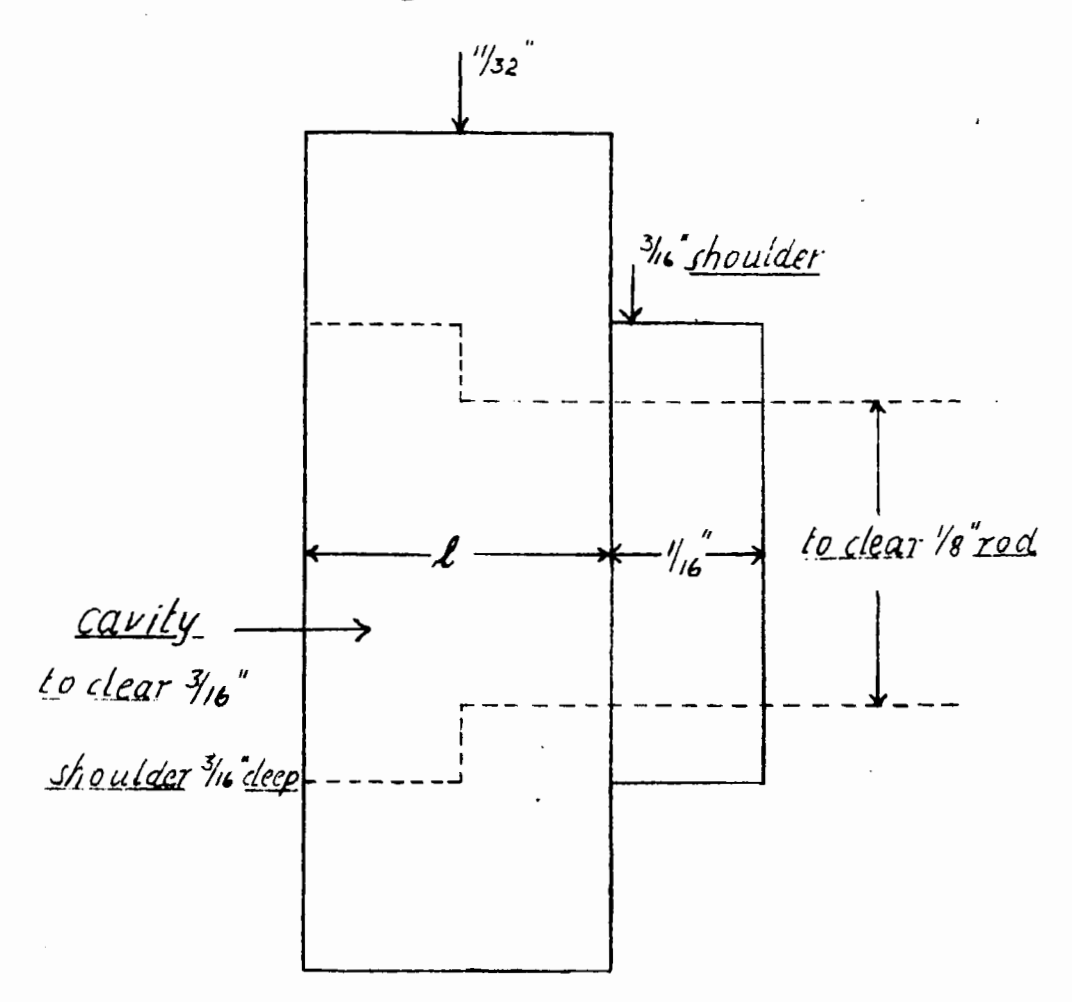
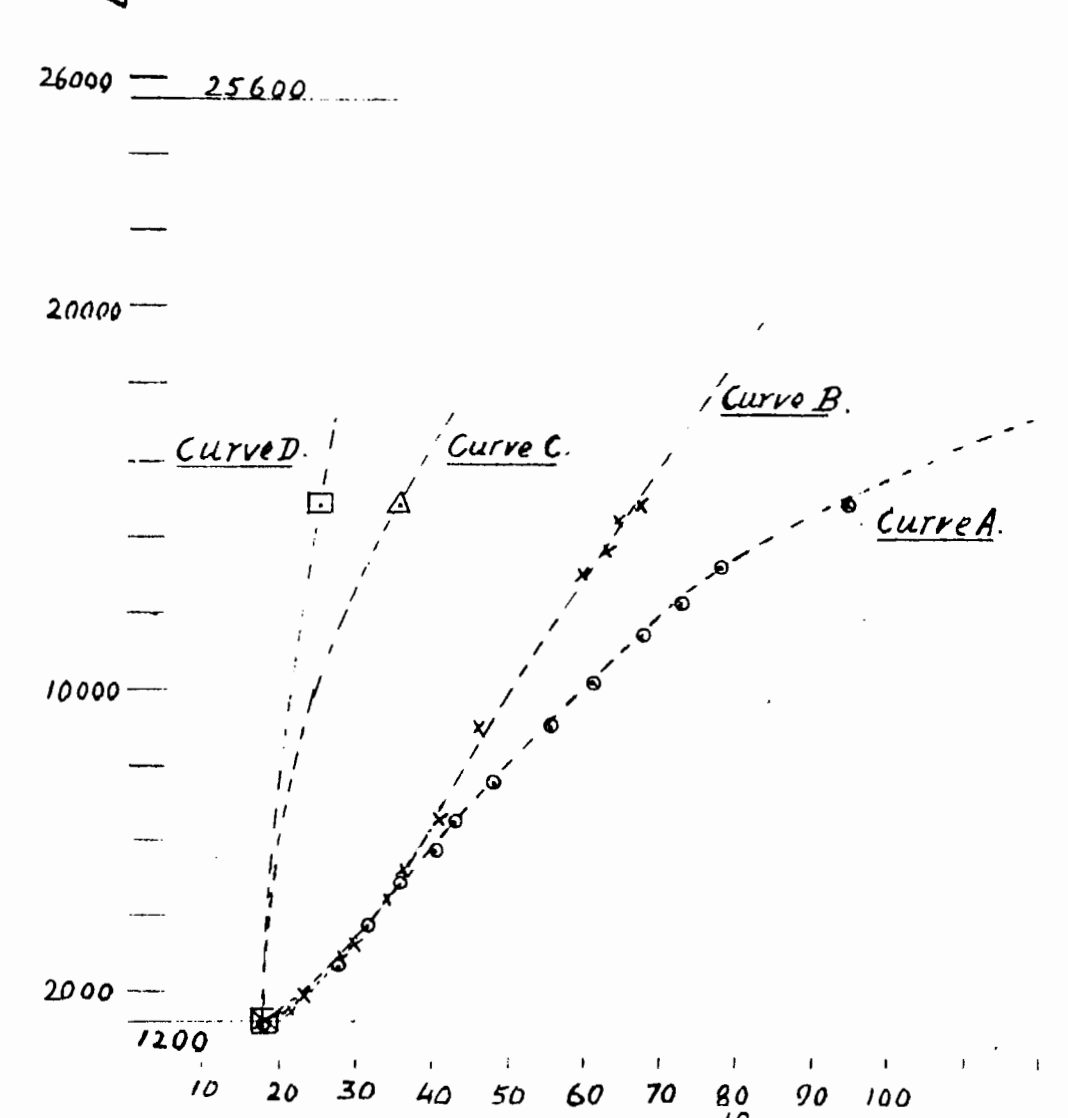


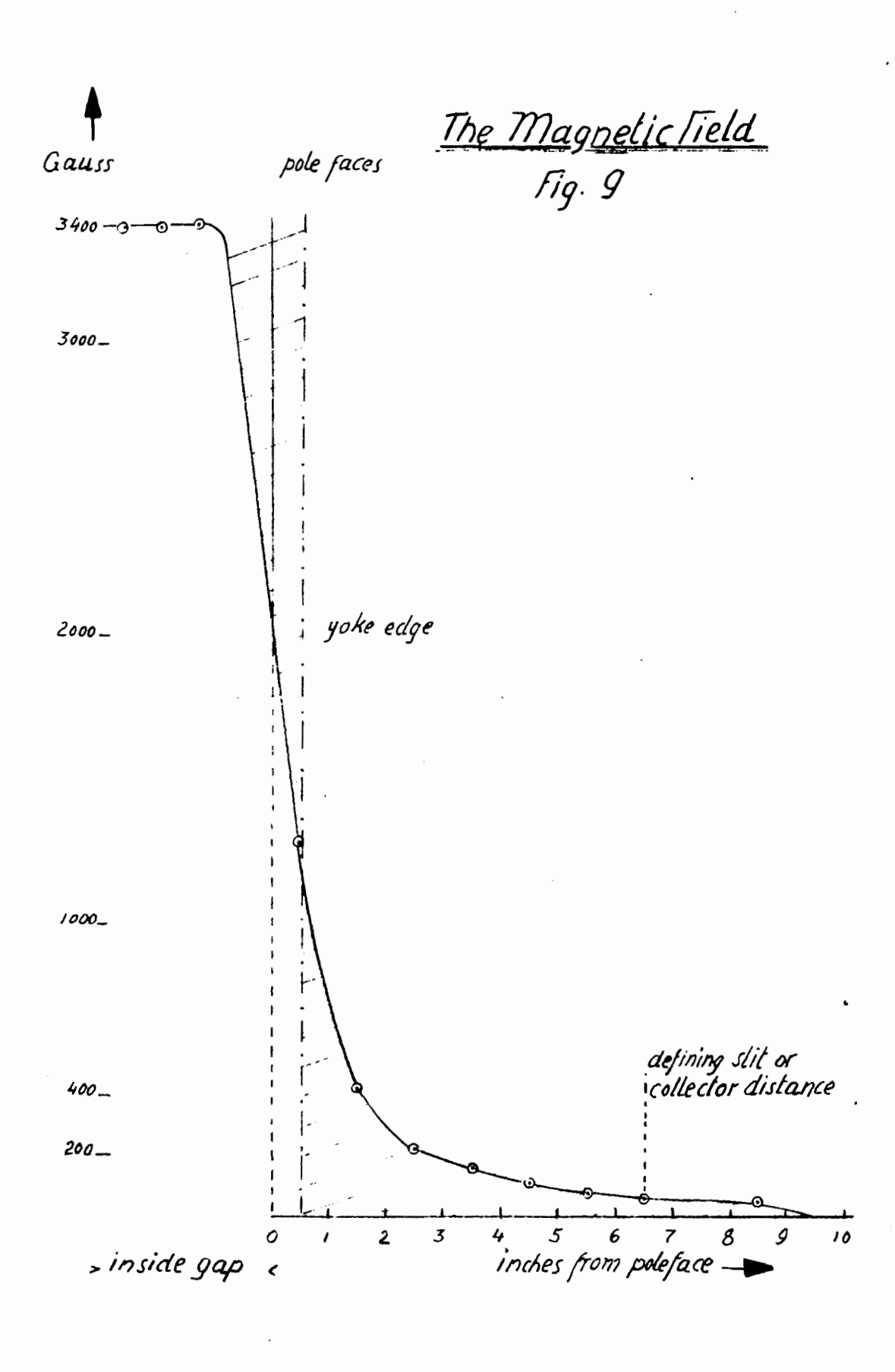
FIGURE 6. Source Holder Mount with Standard Lens

Teston Spacer Fig. 7



Field Emission Effect on Current Fig. 8.





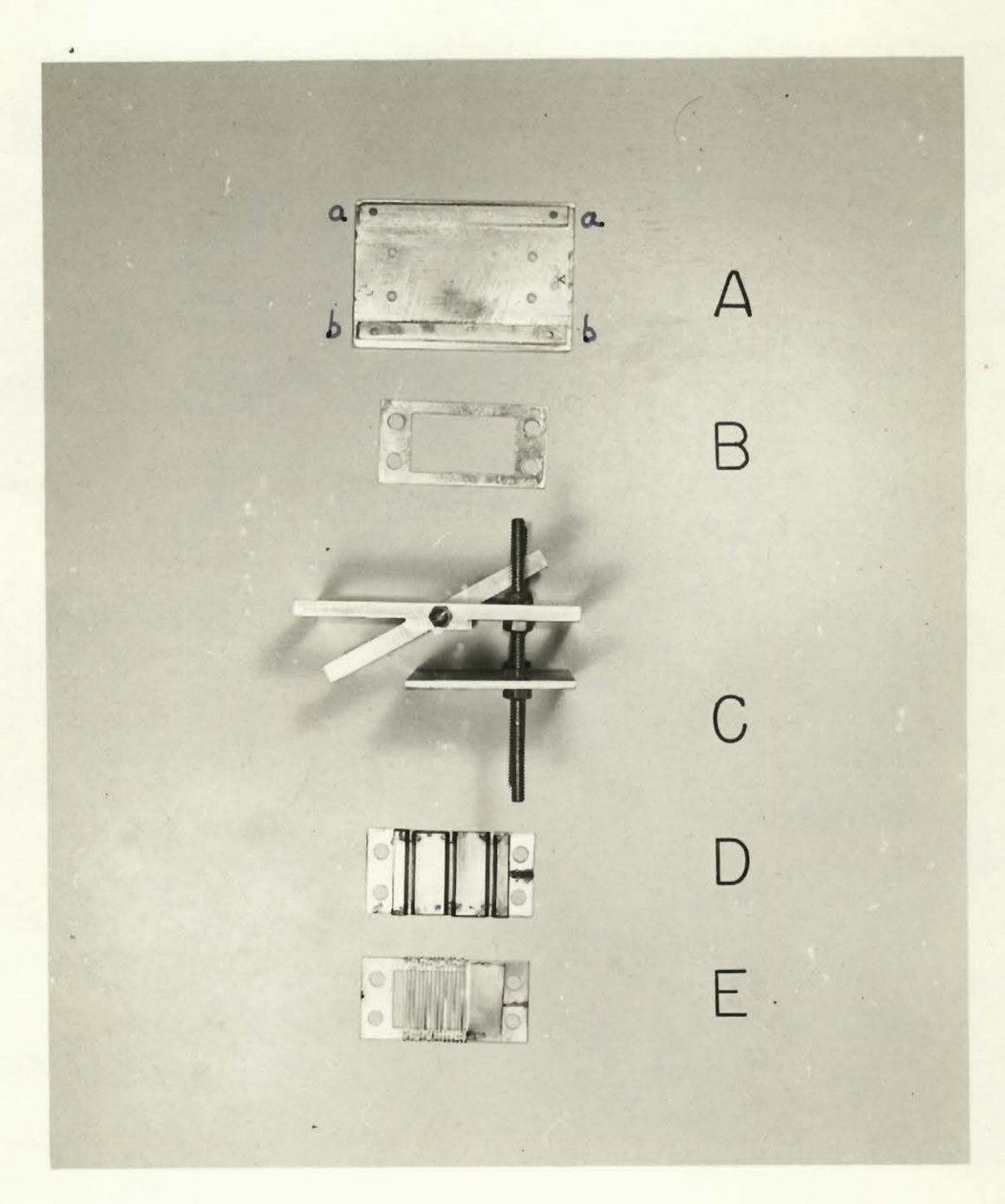


FIGURE 10. Components of the Isotope Collector

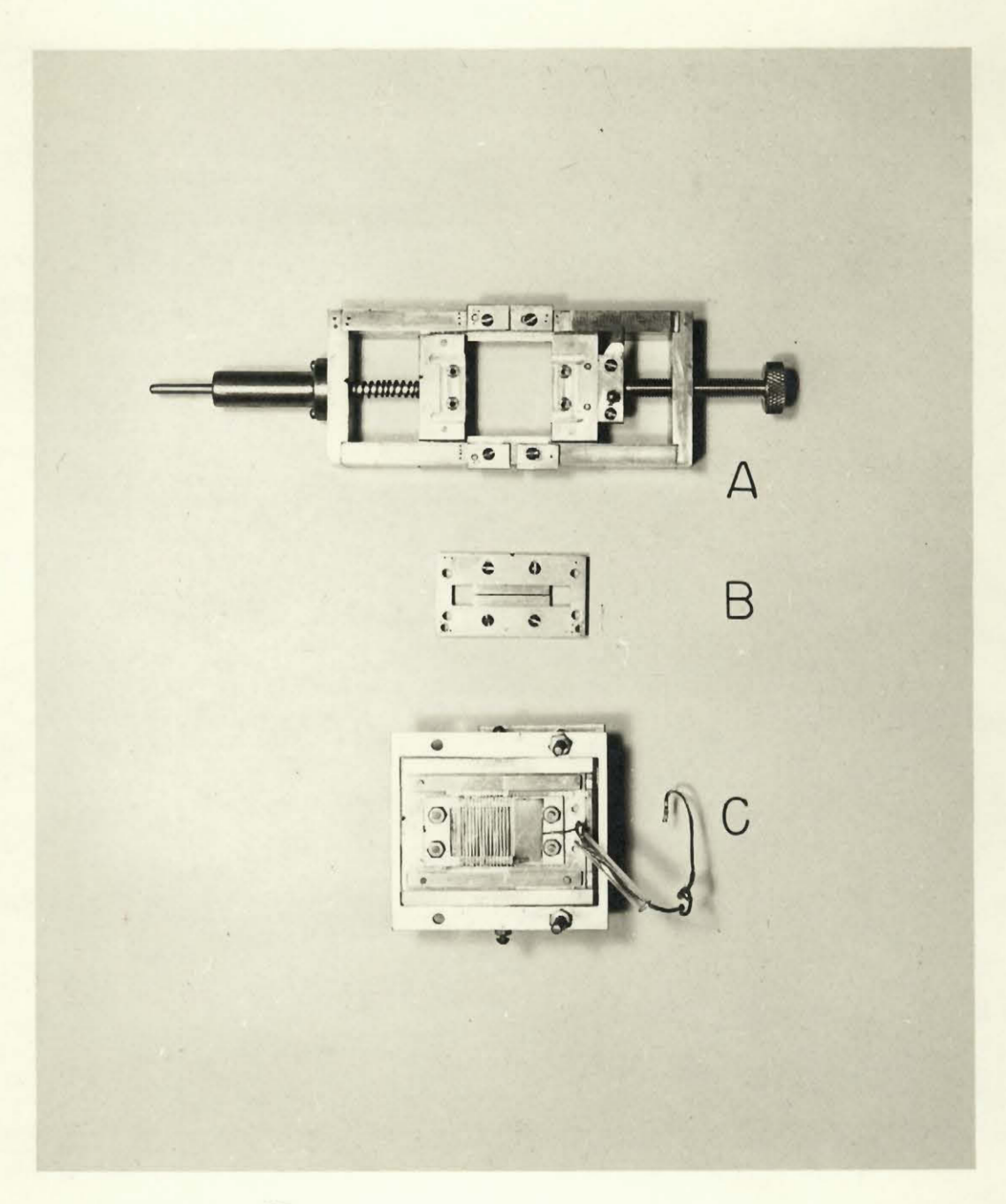
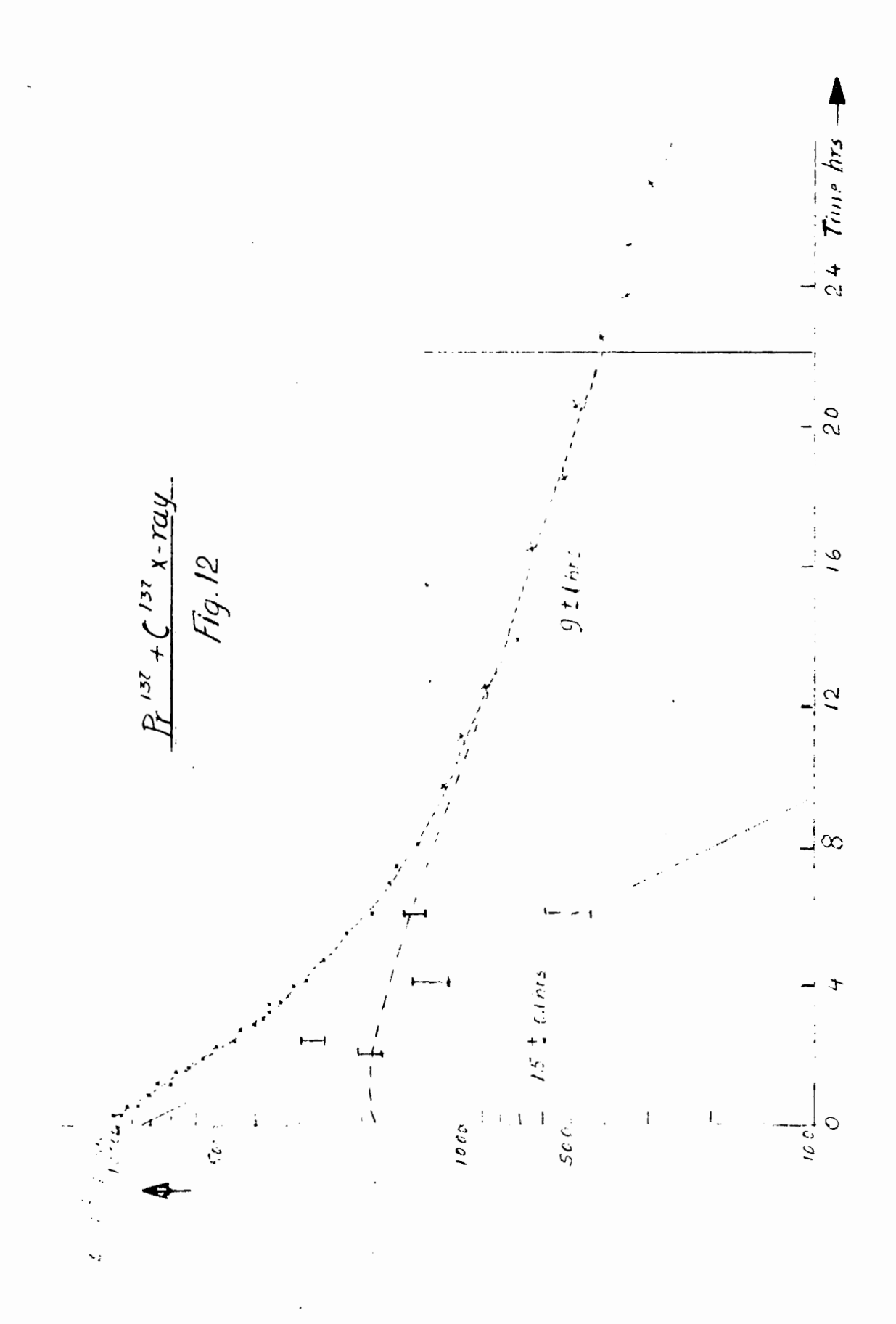


FIGURE 11. Jig and Assembled Collector

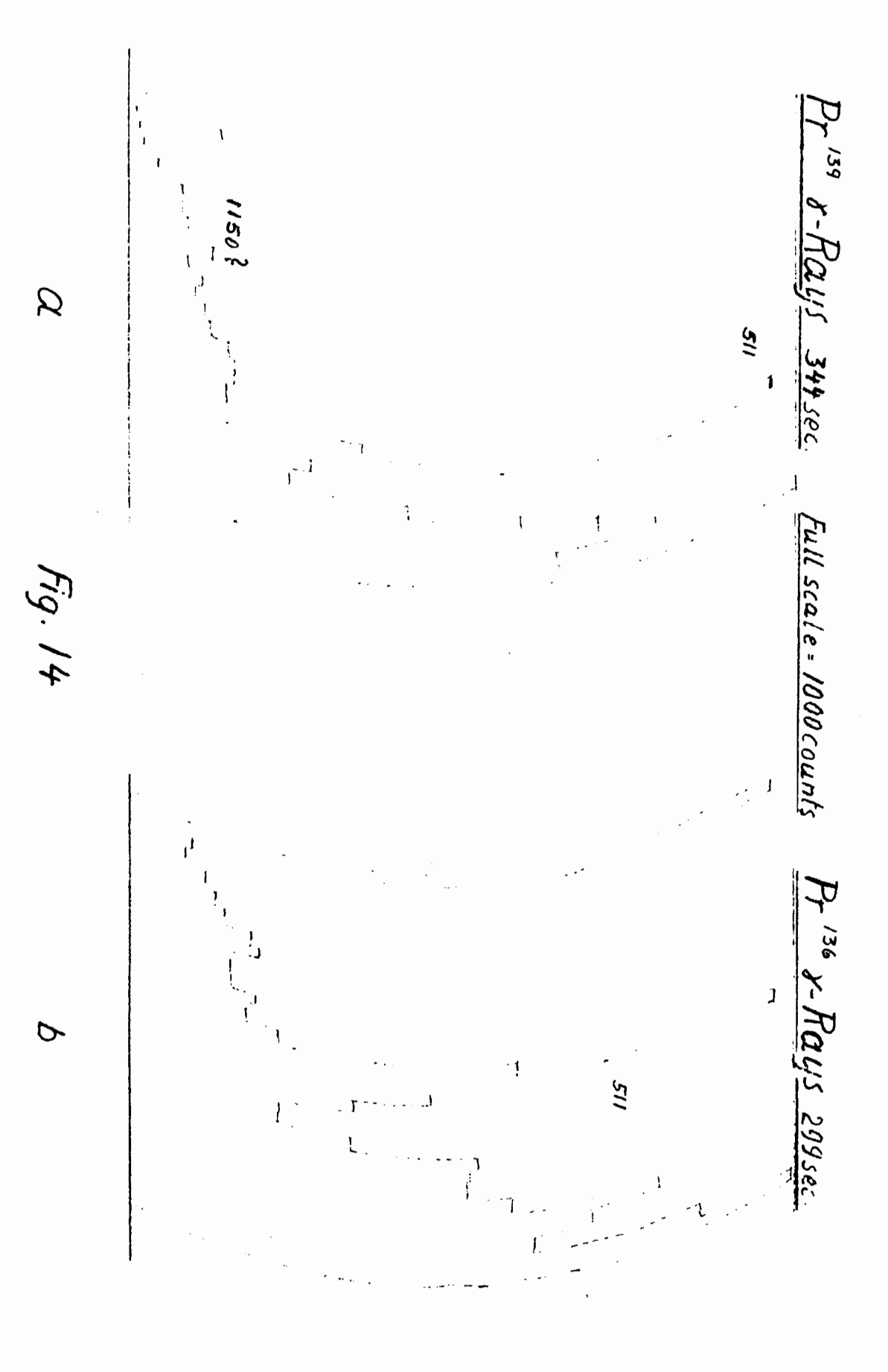


Pr 137 X-Rays 435 sec full scale = 1000 counts Baciground 635 sec

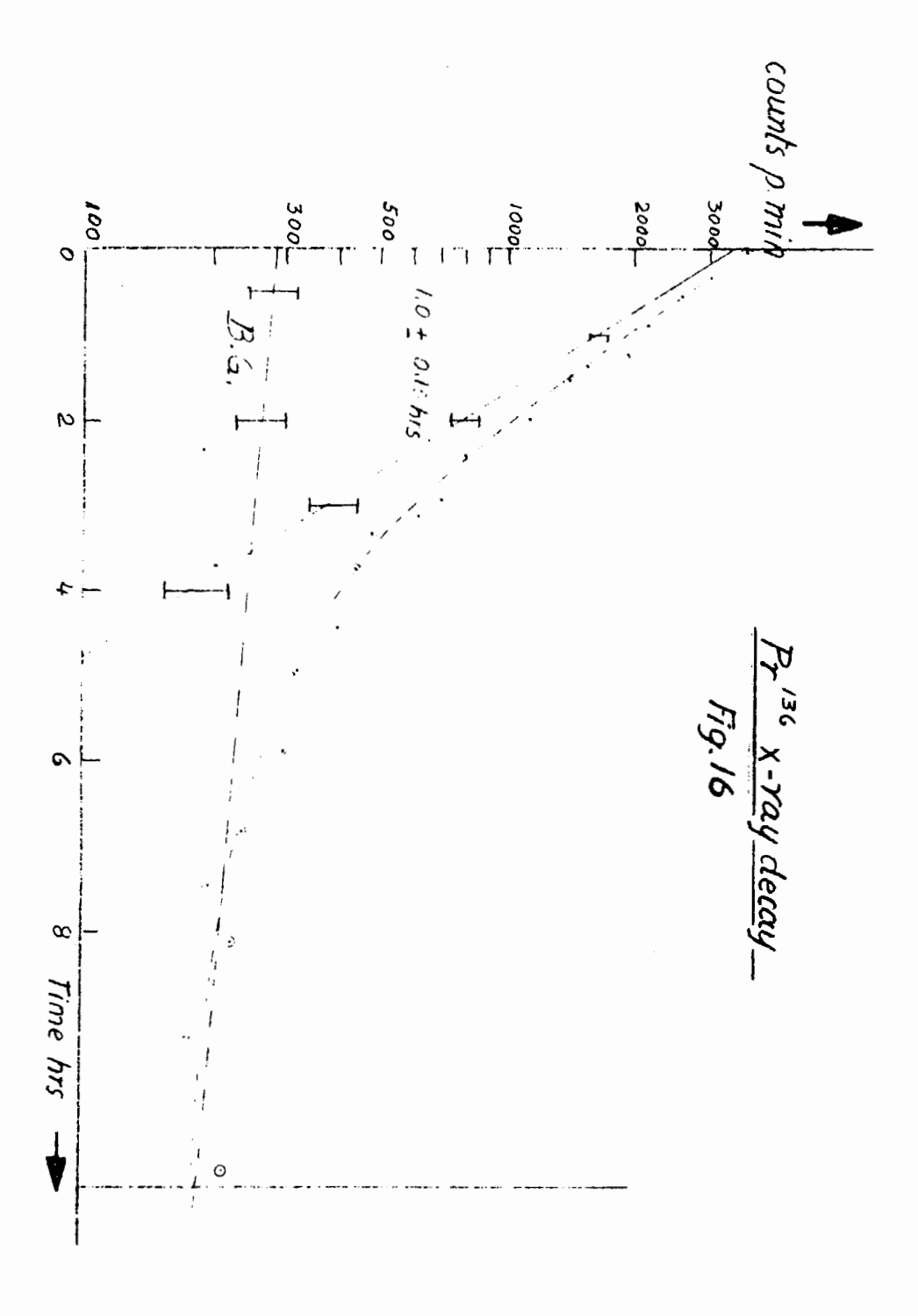
Q

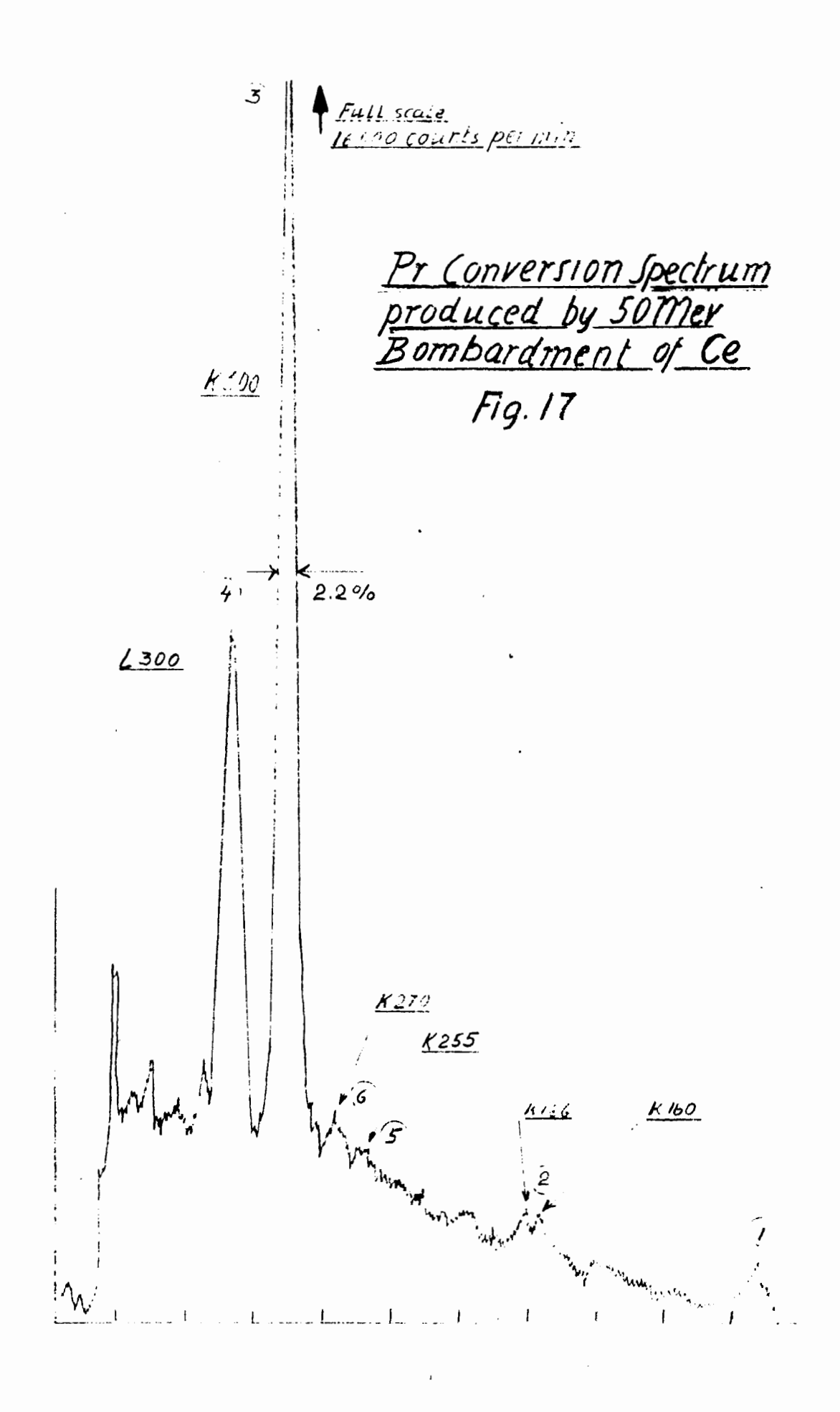
Fig.13

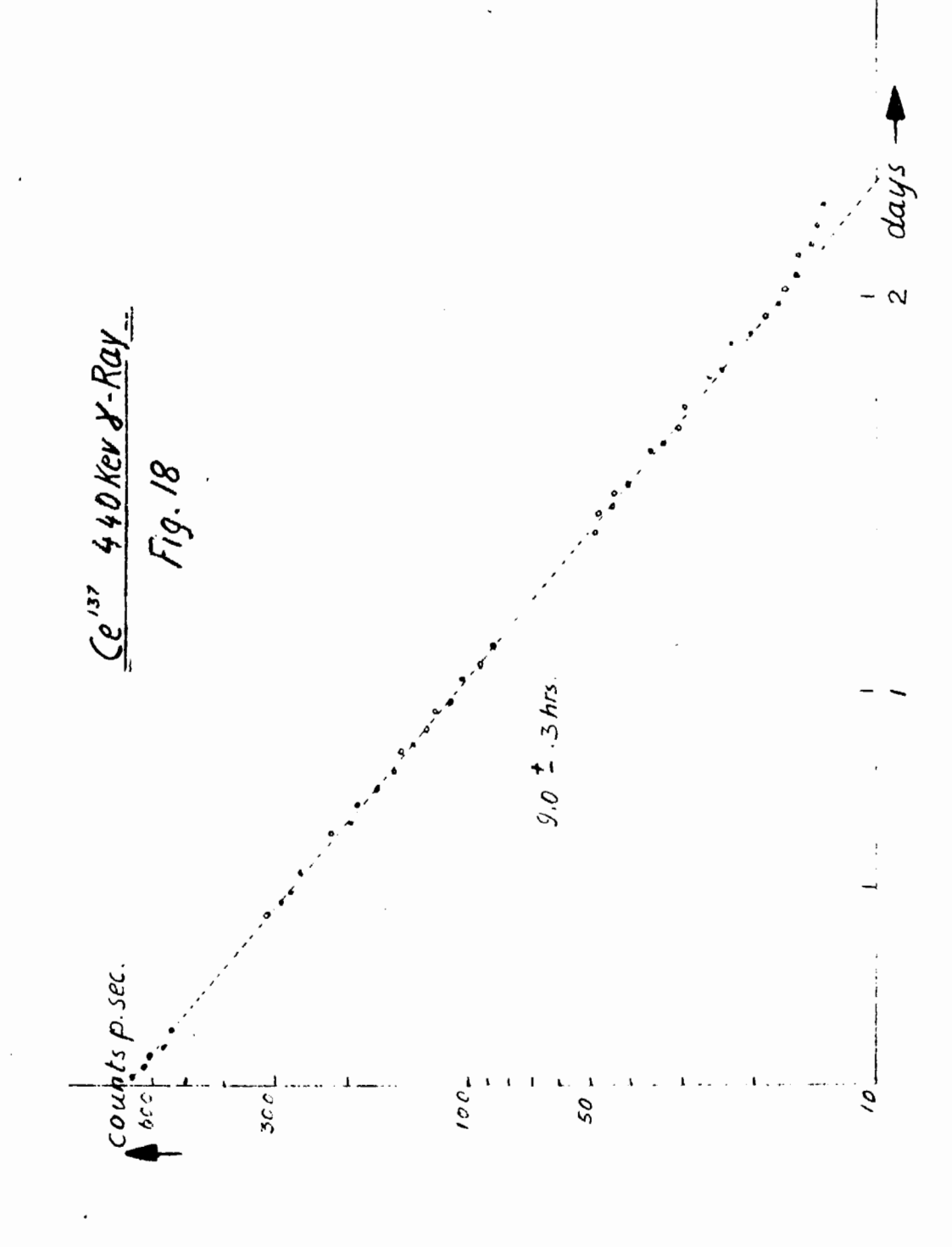
C

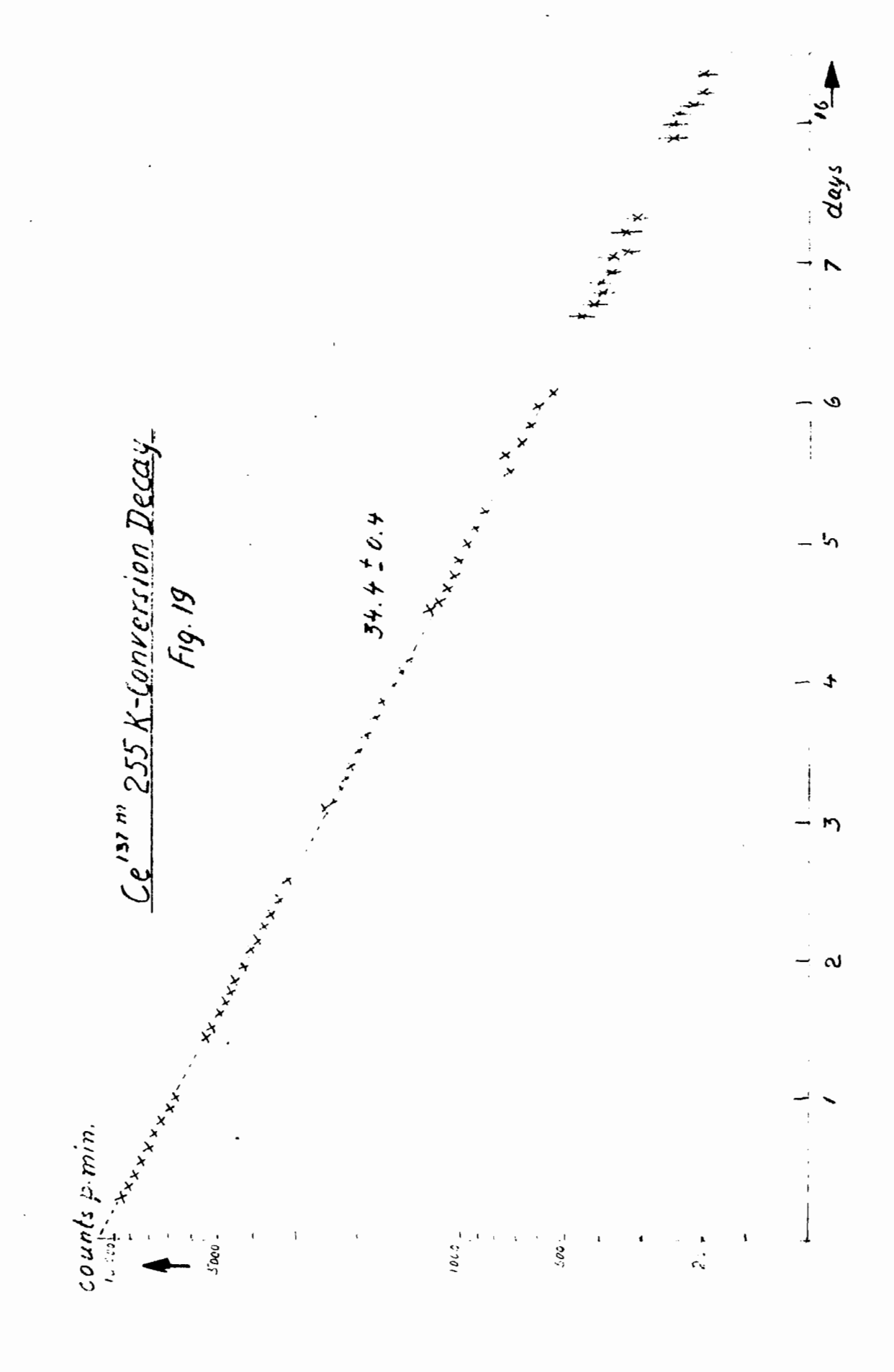


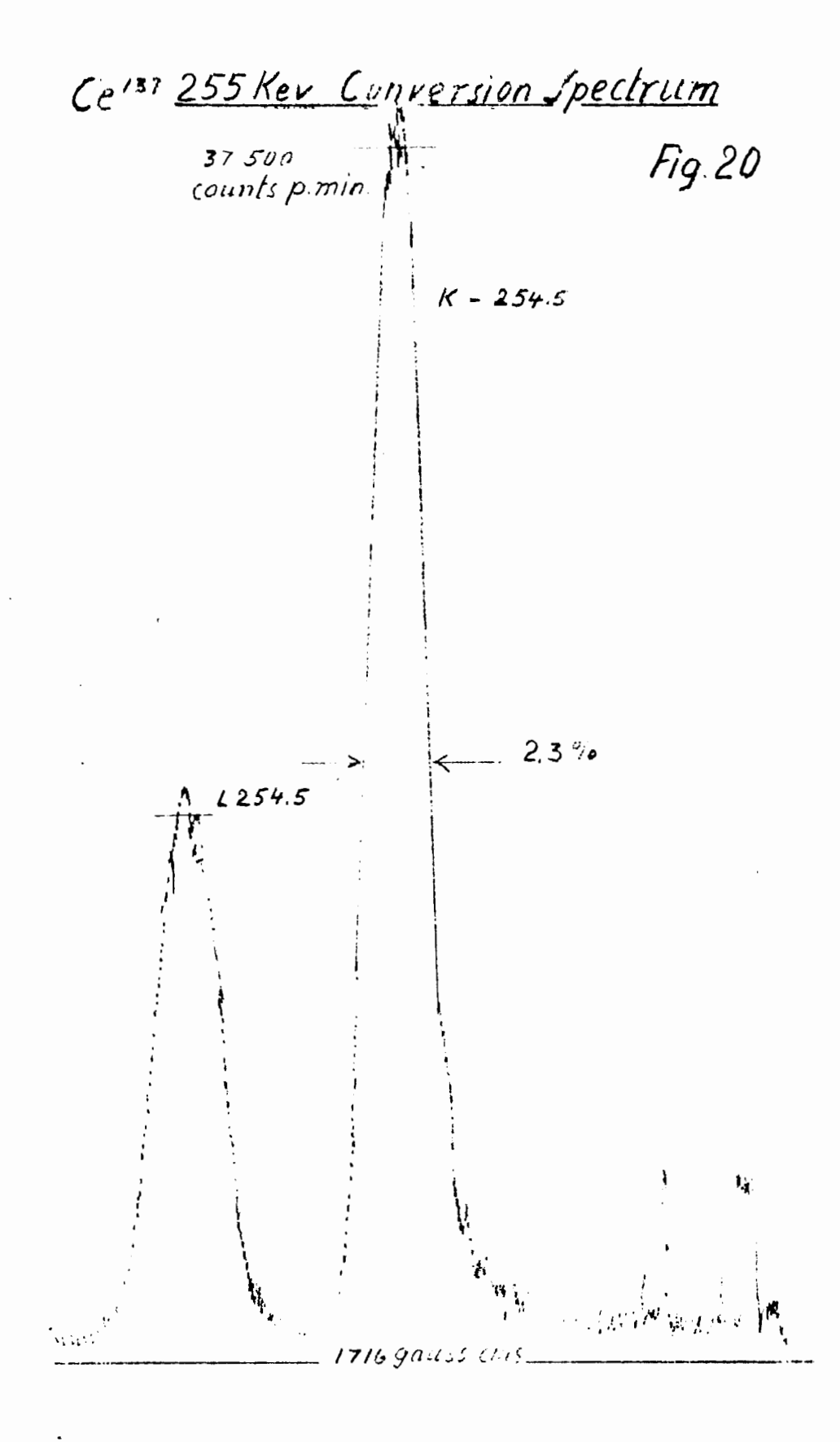
Q



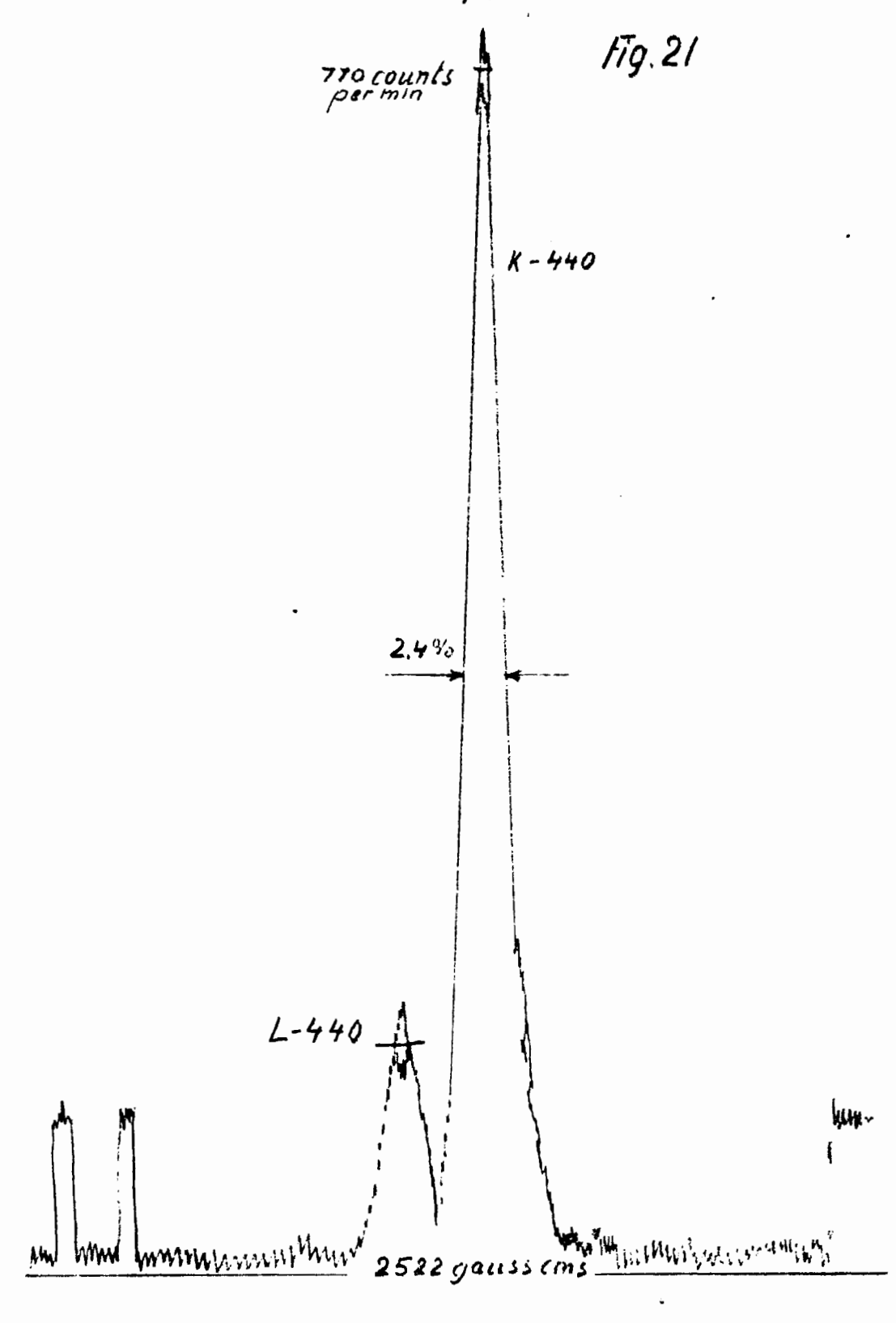








Ce 137 440 Ker Conversion Spectrum





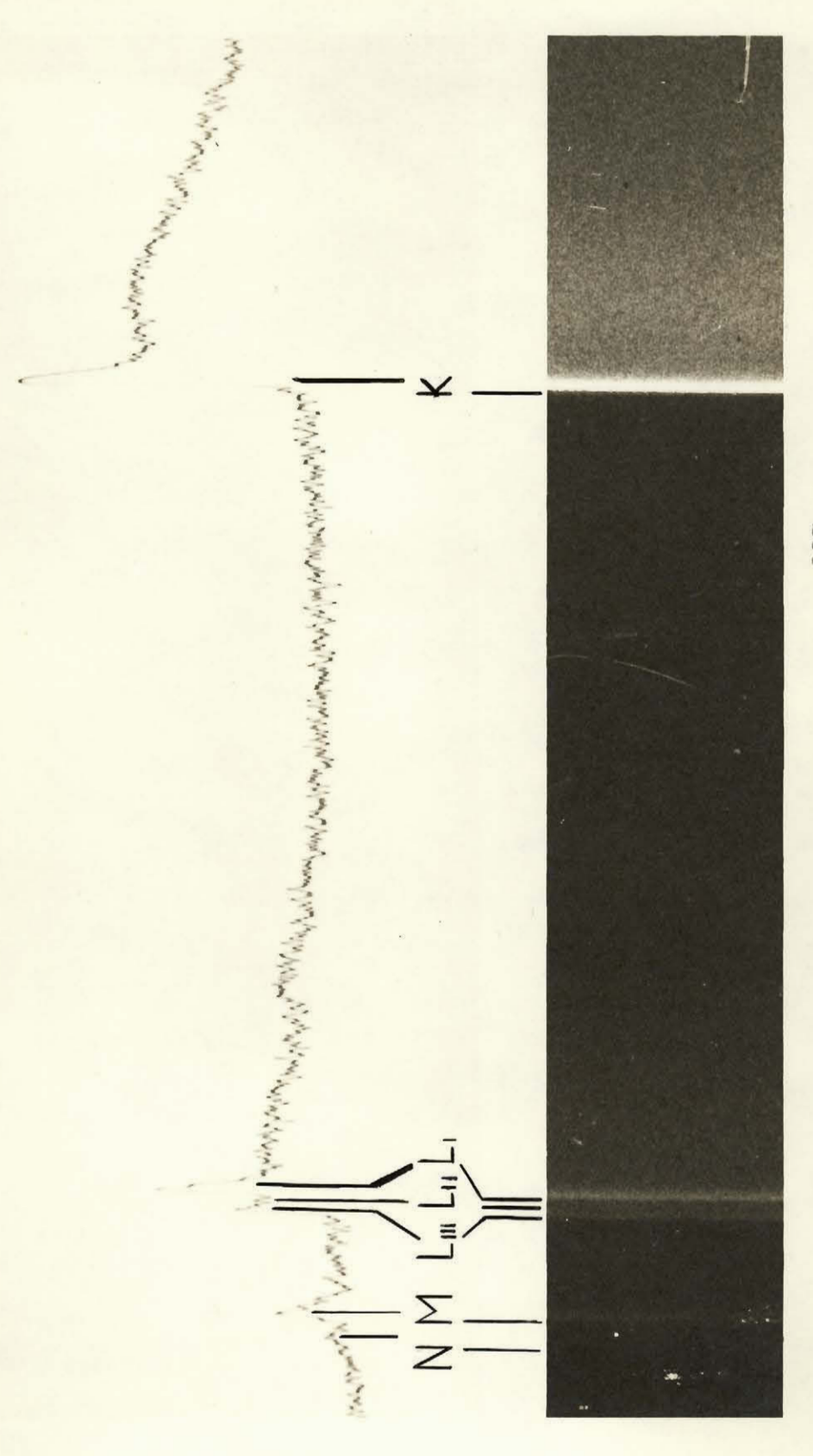
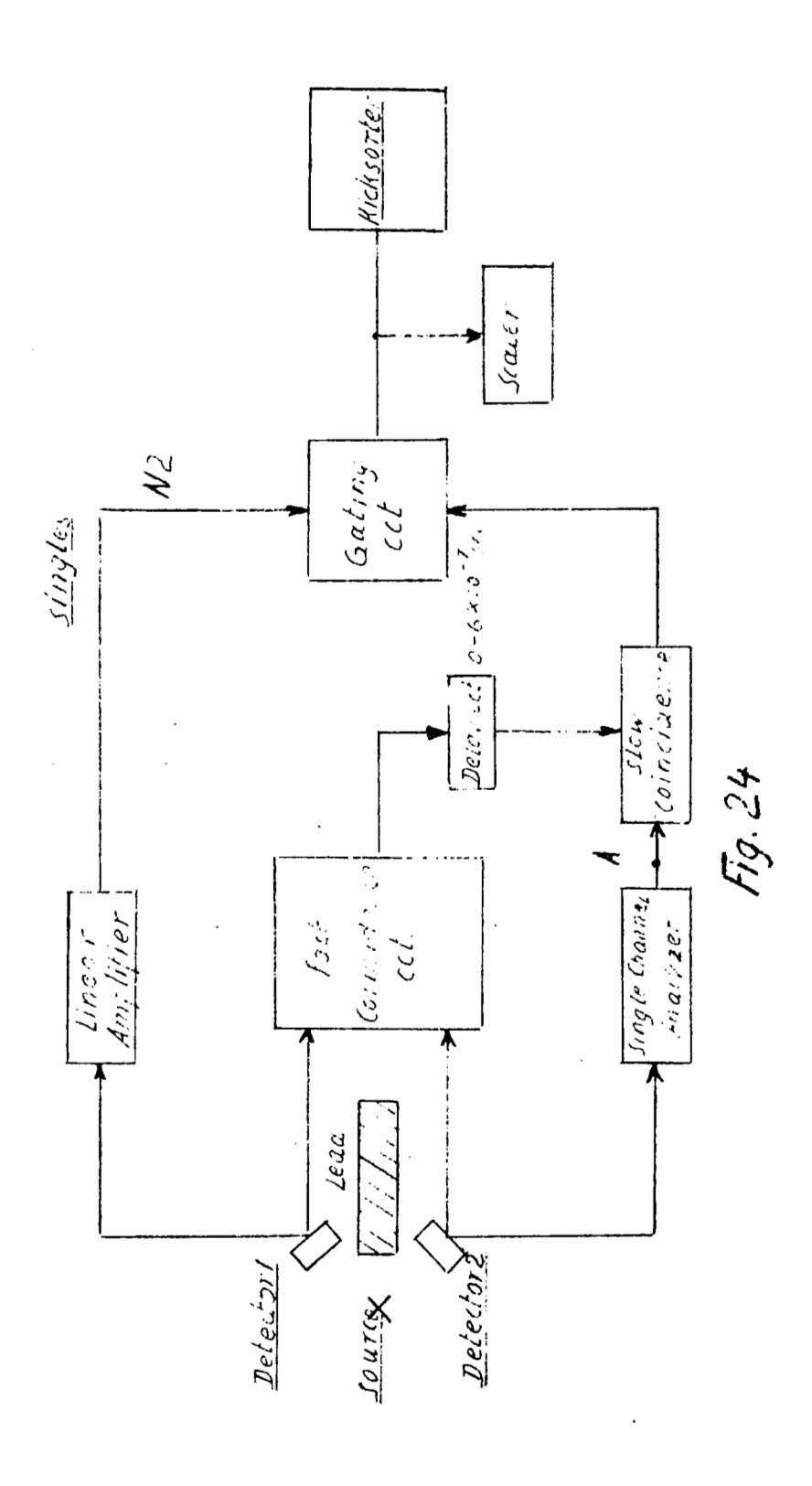
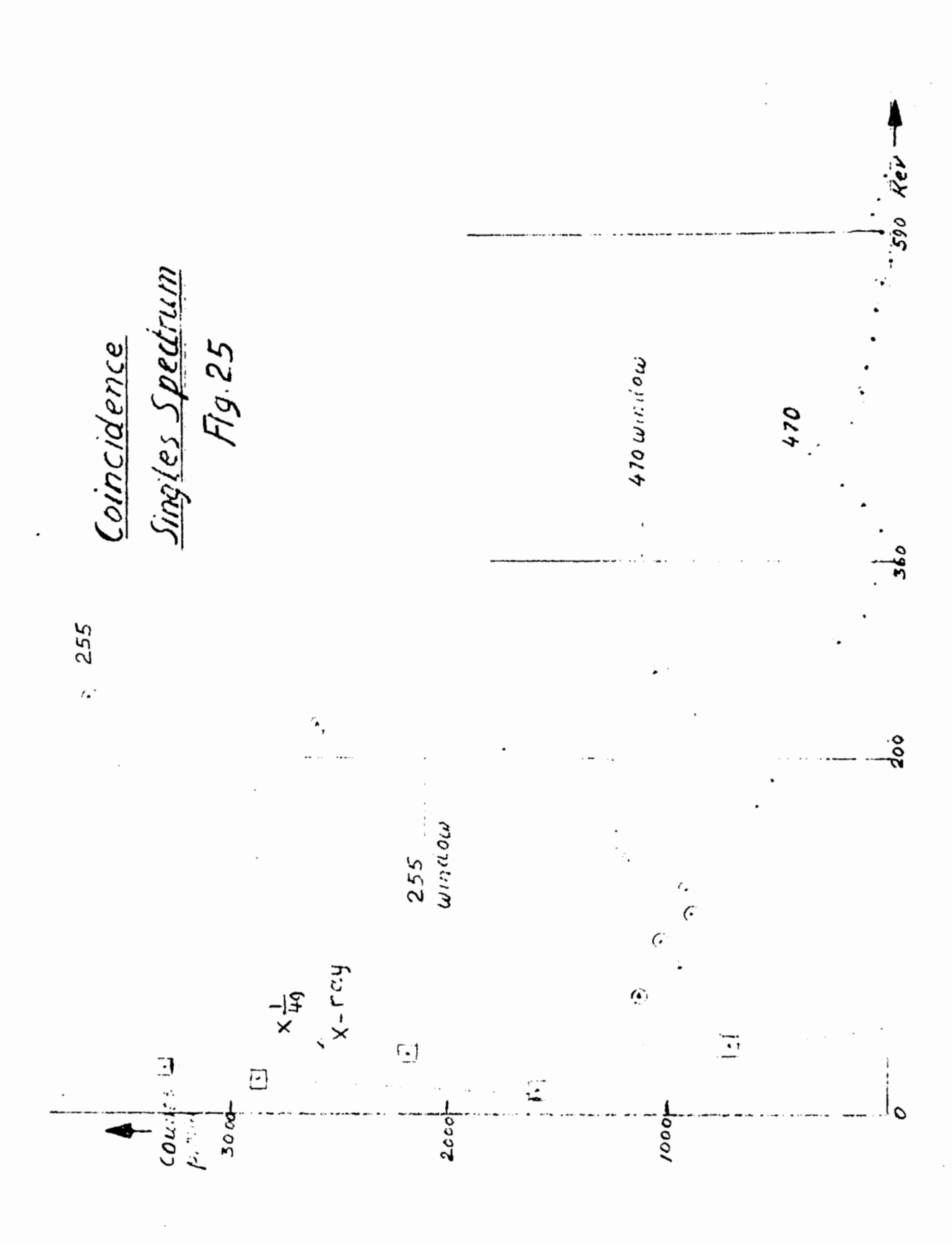
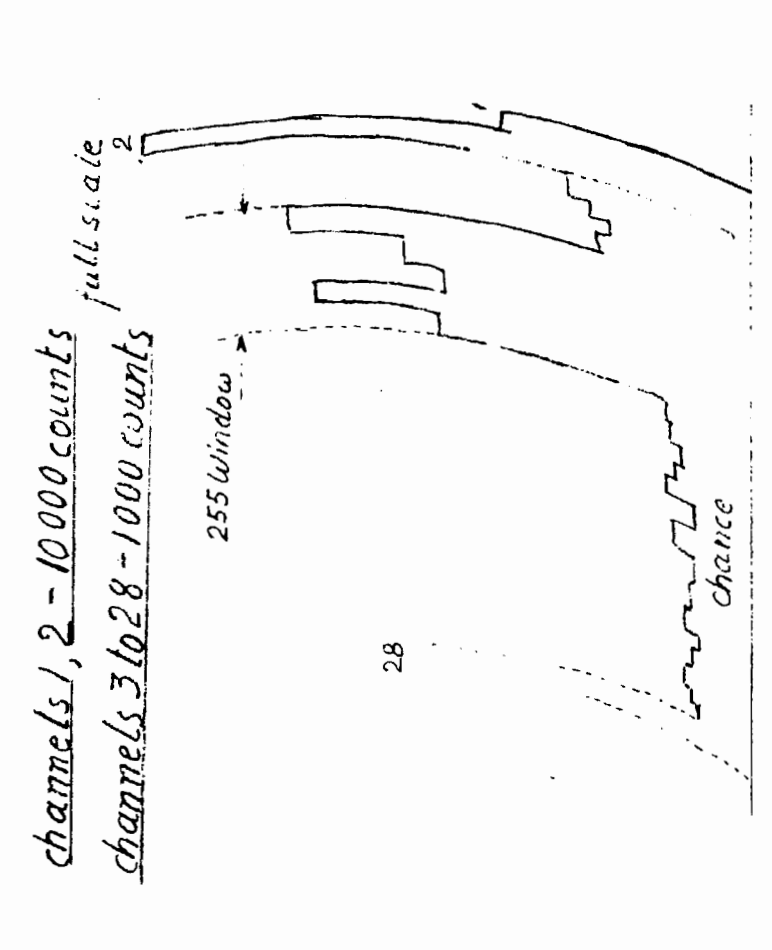


FIGURE 23. Conversion Electron Spectrum of Ce¹³⁷ 255 kev transition







255 Kev Coincidence Spectrum Fig 26

Decay Scheme of 137 Cixuin Fig. 27

~ 2.8 Mer 59 Pr 137

54.4 hrs 58 CC 75 m4 (1 1/2)

. 6 % toca.